ROLE OF HYPOXIA AND HYPOXIA-INDUCIBLE FACTOR-1 IN TUMOUR IMMUNE ESCAPE

by

Xin Li

A thesis submitted to the Department of Anatomy and Cell Biology

In conformity with the requirements for

the degree of Master of Science

Queen's University

Kingston, Ontario, Canada

(August, 2009)

Abstract

Previous studies revealed that, upon exposure to hypoxia, tumour cells acquire resistance to the cytolytic activity of IL-2-activated lymphocytes. The MHC class I chain-related (MIC) molecules – comprised of MICA and MICB – are ligands for the activating NKG2D receptor on Natural Killer (NK) and $CD8^+$ T cells. MIC-NKG2D interactions lead to the activation of NK and $CD8^+$ T cells and the subsequent lysis of the tumour cells. The study also showed that the mechanism of the hypoxia-mediated immune escape involves the shedding of MIC, specifically MICA, from the tumour cell surface. The objective of the present study was to determine whether the shedding of MICA requires the expression of hypoxia inducible factor-1 (HIF-1), a transcription factor that regulates cellular adaptations to hypoxia. Exposure to hypoxia (0.5% O_2 vs. 20% O_2) led to the shedding of MIC from the surface of MDA-MB-231 human breast cancer cells and DU-145 human prostate cancer cells as determined by flow cytometry. Knockdown of HIF-1α mRNA using siRNA technology resulted in inhibition of HIF-1α accumulation under hypoxic conditions as determined by Western blot analysis. Parallel study revealed that knockdown of HIF-1α also blocked the shedding of MICA from the surface of MDA-MB-231 cells exposed to hypoxia. These results indicate that HIF-1 is required for the hypoxia-mediated shedding of MICA and, consequently, that HIF-1 may play an important role in tumour immune escape. Ongoing studies aim to determine the HIF-1 target genes involved in the shedding of MICA under hypoxia.

Acknowledgements

First of all I would like to thank my supervisor Dr. Charles Graham. You are the one who offered me the opportunity to see the other side of the world. I appreciate all your guidance, patience and support over the past two years, and I do consider myself fortunate to be a student of yours and a member of our wonderful lab.

To Rich, Ping, Gail, Genevieve and Steve, thank you for helping me get started with my research program and offering me suggestions whenever I met problems with my experiments. Gail especially, you are such a good teacher to me!

To Shannyn, Genevieve and Janet, thank you for preparing experiment materials for me. Janet especially, thank you for being so invested in my thesis project, both in the experiments and in the thesis-writing, without you I may not graduate on time.

To Dr. Rob Siemens, Dr. Lois Mulligan and Dr Peter Greer, thank you for giving me guidance on my research project and offering me advices to optimize my experiments.

Thank you to Mr. Matthew Gordon, Jalna Meens and Jeff Mewburn (Cancer Research Laboratories) for conducting the flow cytometric analysis.

Finally, I would like to thank my parents and my friends. Your love and support mean so much to me, especially when I am alone here to pursue this Master degree.

Statement of Contribution

Ms. Geneviève C. Paré is to be acknowledged for her contribution of the Real-time PCR analysis shown in Figure 3.9A.

Ms. Janet Elliott is to be acknowledged for her contribution of the Western blot analysis shown in Figure 3.9B

Table of Contents

List of Abbreviation

ADAM……………………………… a disintegrin and metalloproteinase

CI…………………………………… confidence interval

CMK………………………………... chloromethylketone

CTAD……………………………….. C-terminal transactivation domain

DAP10………………………………. DNAX-activating protein of 10 kD

ERp5……………………………….... endoplasmic reticulum protein 5

FIH-1……………………………….... factor inhibiting HIF-1

Grb2…………………………………. growth factor receptor-bound protein 2

HIF-1………………………………… hypoxia inducible factor 1

HRE………………………………….. hypoxia-responsive element

IFN-γ…………………………………. interferon-γ

IGF2………………………………….. insulin-like growth factor-2

MAPK……………………………….... mitogen-activated protein kinase

MCA…………………………………. chemical carcinogen methylcholanthrene

MHC…………………………………. major histocompatibility complex

MIC…………………………………. . MHC class I-chain-related proteins

MICA……………………………….... MHC class I-chain-related protein A

MICB……………………………….... MHC class I-chain-related protein B

mMICA………………………………. membrane-bound MICA

MMPs……………………………….... matrix metalloproteinases

NK cell……………………………….. nature killer cell

NKG2 ………………………………... natural killer group 2

NKG2D …………………………….... natural-killer group 2, member D

ODDD…………………………...… oxygen dependent degradation domain

PBL…………………………….…….. peripheral blood lymphocytes

PCs………………………………….... Pro-protein convertases

PHD………………………………….... prolyl hydroxylase domain containing enzymes

PI3K…………………………………..phosphoinositide-3 kinase

pVHL…………………………………....von Hippel Lindau protein

qPCR …………………………………quantitative PCR

RAET…………………………………the retinoic acid early transcript

SEM…………………………………..standard error of the mean

TCA………………………………......tricarboxylic acid

TGF-α ………………………………...transforming growth factor-α

TRAMP …...…………………………transgenic adenocarcinoma of the mouse prostate

ULBPs………………………………..UL16-binding proteins

VEGF…………………………………vascular endothelial cell growth factor

List of Figures

List of Tables

Chapter 1

Introduction

1.1 Cancer Immunology

1.1.1 Host-protecting effect of the immune system against developing tumours

Cancer immunosurveillance is defined as immunological protection of the host against the development of cancer, resulting from immune effector functions stimulated by immune recognition of either stress ligands or antigens expressed on transformed cells [1].

The concept of immunosurveillance was first proposed by Burnet and Thomas in the 1950s. However, subsequent studies in the 1970s comparing wild type with athymic nude mice failed to show either increased incidence of chemically induced tumours or a shortened tumour latency period after carcinogen injection in these immune-deficient mice [2]. Furthermore, there were no statistically significant differences in the incidence of spontaneous non-viral tumour formation between nude and wild type mice. Due to the limited understanding at that time of the immunological defects in the nude mouse, these results were considered to be highly convincing and consequently led to the abandonment of the immunosurveillance hypothesis [3, 4].

Between 1994 and 1998, two major findings led to the renewed interest in the process of cancer immunosurveillance: endogenously produced interferon γ (IFN-γ) could protect the host against the growth of transplanted tumours and against the formation of primary chemically-induced and spontaneous tumours, and that mice lacking the cytolytic protein perforin were more prone to tumour induction by the chemical carcinogen methylcholanthrene (MCA) compared with their wild type counterparts [4]. Recent studies using mice with molecularly defined inactivating defects in innate and/or adaptive immunity have together shown that immunodeficiency does indeed lead to increased incidence of spontaneous and carcinogen-induced tumours. These data now give strong support for the existence of an effective cancer-immunosurveillance mechanism in mice. Moreover, clinical data indicate that cancer immunosurveillance also occurs in humans: studies of transplant recipients who were immune-suppressed and of individuals with primary immune-deficiencies showed that both groups had a significantly higher risk for cancer development than the general population [1, 4-6].

1.1.2 Tumour-sculpting role of the immune system

Since cancer occurs in immune-competent individuals, it has been thought that during tumour formation, the immune system selects tumour variants that can be best suited to survive in an immunologically intact environment, very like what the immune system does with viruses, bacteria and parasites [4]. Immunoselective effects have been observed as re-passage of transplantable tumours through immune-competent hosts resulted in the predominance of tumour variants with reduced immunogenicity [4]. Moreover, studies have shown that tumours from immunocompetent hosts and immunodeficient hosts have different immunogenic phenotypes: tumour cells taken from immunocompetent mice could form progressively growing tumours when transplanted into immunocompetent recipients, whereas tumour cells taken from immunodeficient mice were rejected when transplanted into wild-type hosts [1, 7-9].

1.1.3 Cancer immunoediting

The opposing functions of immunity — host protection versus tumour sculpting — form the basis for a process termed cancer immunoediting [4].

This process consists of three phases: elimination, equilibrium, and escape. In the elimination phase, which corresponds to immunosurveillance, if the inhibition of tumour development and/or growth by immunosurveillance is incomplete, the cancer-immunoediting process can advance to the equilibrium phase. This second phase, which is similar to the older concept of tumour dormancy, is characterized by the persistence of residual cancer cells that are highly mutable. In the escape phase of the cancer-immunoediting process, cancer cells that develop the capacity to avoid destruction by immune responses and/or are able to directly attenuate the protective anti-tumour functions of immune effectors can grow progressively to form clinically evident lesions [1,4]. It is believed that the activating receptor NKG2D (natural-killer group 2, member D) and its ligands play an important role during both the elimination phase and the escape phase of the cancer-immunoediting process.

1.2 NKG2D-NKG2DL interactions during innate immunity

The activating receptor NKG2D was identified in a screen for the preferentially expressed genes by human natural killer (NK) cells [10-12]. It was designated as NKG2D as its gene resides in the NKG2 (natural killer group 2) complex. Expression of this activating receptor was shown in NK cells, most NKT cells, $\gamma\delta^{+}$ T cells, and $CD8^{+}$ T cells. Under non-pathological conditions, expression of NKG2D is not detectable on a substantial proportion of $CD4^{+}$ T cells [13-20].

The NKG2D receptor binds to a variety of ligands, which resemble major histocompatibility complex (MHC) class I proteins [20-23]. In humans, NKG2D ligands consist of the Retinoic Acid Early Transcript 1 (RAET1) family members, which were initially referred to as UL16-binding proteins (ULBPs), and the MHC class I-chain-related (MIC) proteins A and B. The members of the RAET1 family of ligands are orthologues of the mouse RAE-1 proteins, containing $\alpha1$ and $\alpha2$ domains; while the MIC family has a third Ig-like domain $\alpha3$ [21, 24, 25].

Ligands for NKG2D are rarely detectable on the surface of healthy cells and tissues, but their expression can be up-regulated by many factors, including infection by bacteria or viruses or by cellular transformation [20]. They are frequently expressed by tumour cell lines and in tumour tissues. It has been reported that RAET1 proteins are expressed by tumours of various origin, including leukemias, gliomas and melanomas [20, 26-28], while MICs are even more broadly expressed in leukemias, various carcinomas (breast, lung, colon, kidney, ovary and prostate), gliomas, neuroblastomas and melanomas [20, 26-32].

Interactions between NKG2D and NKG2DLs can lead to the activation of NK cells despite the presence of inhibitory signals induced by the expression of MHC class I molecules on target cells [21, 33]. NKG2D-NKG2DL interactions can also co-stimulate $CD8^+$ T cell activation [20]. Specifically, NKG2D does not contain any known signalling motifs within its intracellular domain. Upon binding to a ligand, NKG2D associates with the adaptor protein DNAX-activating protein of 10 kD (DAP10). The latter carries a Tyr-X-X-Met motif within the cytoplasmic domain, which then recruits phosphoinositide-3 kinase (PI3K) and growth factor receptor-bound protein 2 (Grb2) [20]. In NK cells, the subsequent downstream signalling triggers cell degranulation, with release of perforin and granzymes at the junction between the interacting cells. Granzyme B enters the target cell via perforin-gated pores or by binding to mannose 6-phosphate receptors that are subsequently endocytosed. Granzyme B is then released from the vesicle into the cytoplasm in a perforin-dependent process [34]. Cleavage of procaspase 8 by granzyme B activates a caspase cascade that leads to the apoptotic death of the NKG2D ligand-bearing targets [34]. Thus during the process of tumourigenesis, NKG2D-NKG2DL interaction plays an important role in the NK-mediated immune response.

Among NKG2DL members, MICA was the first identified and is the most extensively studied. MICA is highly polymorphic, as it has 61 known alleles. As mentioned above, MICA is not expressed on the surface of most normal tissues except on the intestinal epithelium and its expression can be enhanced in virus- or bacteria-infected cells or in tumour cells[20]. It was reported that an AP-1-binding site is present in the promoter region of the *MICA* gene [35]. AP-1 is a transcription factor that mediates gene regulation in response to a variety of extracellular stimuli including growth factors, cytokines, oncogenes, tumour promoters and chemical carcinogens [36]. AP-1 plays an important role during tumourigenesis as it is involved in the regulation of cell proliferation, differentiation and apoptosis [36]. At the same time, it is well established that the DNA damage pathway is activated in many tumours, and DNA damage can induce surface expression of MICA [37]. Thus it has been proposed that AP-1 and the DNA damage pathway cooperate in the up-regulation of MICA during tumourigenesis [20]. High levels of soluble MICA were detected in sera of patients suffering from different types of cancer, including breast and lung cancer, leukemia, pancreatic carcinomas, hepatocellular cancer and colon carcinoma [28, 38-41]. There is also evidence that soluble MICA is an independent marker of progression for many early-stage cancers, such as gastrointestinal, breast, and prostate carcinoma [20, 42]. The shedding of MICA is mediated by metalloproteinases; one study has shown that MICA shedding by tumour cells was inhibited by the silencing of ADAM-10 and ADAM-17, two members of the "a disintegrin and metalloproteinase" (ADAM) family of metalloproteinases [43]. Cell surface endoplasmic reticulum protein 5 (ERp5) is also required for MICA shedding: it acts by forming mixed disulfide complexes that release MICA [44]. It has been proposed that shedding of MICA may have multiple consequences on NKG2D-mediated responses: first, shedding of MICA itself reduces MICA density on the tumour cell surface; second, soluble MICA can down-regulate expression of NKG2D on effector cells; and third, soluble MICA can bind to the NKG2D receptor thereby blocking interactions between NKG2D and NKG2D ligands on the cell membrane [20].

1.3 Hypoxia and tumour cell biology

Growth of a solid tumour is limited by the extent of vascularisation which supplies tumour cells with oxygen and nutrients [45]. Because of the highly irregular nature of tumour vascular networks, oxygen distribution in human tumours is heterogeneous. Tumour hypoxia (low oxygen tension) usually occurs at a distance of 100–200 μm from blood vessels [46]. Most solid tumours contain regions with pO_2 values of less than 5 mmHg (corresponding to approximately 0.7% O_2 in the gas phase or 7 μM in solution), while the partial pressure of oxygen of normal tissues from which the tumours arose is around 30-50mmHg (corresponding to approximately 4-7% O_2 in the gas phase) (Table 1.1) [45,46].

Hypoxia has a so-called Janus face on tumour progression: it can induce apoptosis (programmed cell death) or necrosis in cells that cannot adapt to oxygen and nutrient deprivation, but it can also prevent cell death by inducing adaptive responses that facilitate cell proliferation or angiogenesis, finally contributing to tumour progression [45].

Hypoxia can hinder or even completely inhibit tumour cell proliferation [47]. It has also been established that hypoxia can induce apoptosis of normal or neoplastic cells via both Hypoxia Inducible Factor-1 in a p53-dependent or p53-independent pathway involving genes such as those of the *Bcl-2* family[45]. Hypoxia-induced differentiation, apoptosis, and necrosis may explain the phenomenon of delayed recurrences, dormant micro-metastases, and growth retardation which can occur in large tumours [46].

In contrast, other studies have revealed that the presence of hypoxia within the tumour mass is correlated with a negative clinical outcome for patients with various types of cancers including carcinoma of the head and neck, soft tissue sarcoma, carcinoma of the cervix, and prostatic adenocarcinoma [48-53]. Some of these studies demonstrated that the survival of patients with severely hypoxic tumours is significantly lower than that for patients with well-oxygenated tumours [47]. Other studies showed that tumour hypoxia is associated with resistance to radiotherapy, chemotherapy, photodynamic therapy and immunotherapy [46, 47]. Hypoxic cells are considered to be resistant to most anticancer drugs for reasons such as inadequate exposure to the anticancer drugs due to long distance from blood vessels, selection of cells that have lost sensitivity to p53-mediated apoptosis, and up-regulation of genes involved in drug resistance [46, 54-56].

In addition, it has been demonstrated that hypoxia in tumours tends to select for a more malignant phenotype: it increases mutation rates, increases expression of genes associated with angiogenesis and invasion, and is associated with a more metastatic phenotype [46]. Thus hypoxia-induced adaptive responses can enable cells to overcome nutrient deprivation, to escape from the hostile local micro-environment, and to acquire clinically aggressive/malignant phenotypes [46].

Since hypoxia and hypoxia-induced necrosis is a unique feature of solid tumours it could potentially be exploited in cancer therapy [46]. Four general strategies are now being developed: using pro-drugs activated by hypoxia, in which a non-toxic pro-drug can be activated to a toxic drug in a hypoxic environment; using hypoxia-selective gene therapy, in which hypoxia-specific promoters provide selective transcription of enzymes that can convert pro-drugs into toxic drugs; targeting the hypoxia inducible factor 1 (HIF-1) transcription factor, the primary factor that mediates cellular adaptations to hypoxia; and using recombinant obligate anaerobic bacteria, in which an obligate anaerobe colonizes a tumour and causes necrosis after systemic administration [46].

Studies from our laboratory showed that hypoxia induces the shedding of membrane-bound MICA (mMICA) from the surface of DU-145 human prostate cancer cells, and increases the resistance of these cells to the lysis mediated by IL-2-activated peripheral blood lymphocytes (PBL). A causal relationship between hypoxia-induced MICA shedding and resistance to PBL-mediated lysis was implied by results which showed that, in the presence of an anti-MICA/MICB antibody which prevents MIC-NKG2D interactions, the sensitivity to the cytolytic activity of donor PBLs was significantly decreased in DU-145 cells pre-incubated in 20% O_2, while addition of anti-MICA/MICB antibody did not further decrease the sensitivity to PBL-mediated cytotoxicity in DU-145 cells pre-incubated in 0.5% O_2 [57].

Table 1.1 Oxygenation of tumours and the surrounding normal tissue

Tumour type	Median tumour pO_2 * (number of patients)	Median normal pO_2 * (number of patients)
Breast cancer	10.0 (15)	ND
Prostate cancer	2.4 (59)	30.0 (59)
Glioblastoma	4.9 (10) 5.6 (14)	ND ND
Head and neck carcinoma	12.2 (30) 14.7 (23) 14.6 (65)	40.0 (14) 43.8 (30) 51.2 (65)
Pancreatic cancer	2.7 (7)	51.6 (7)
Cervical cancer	5.0 (8) 5.0 (74) 3 (86)	51 (8) ND ND

*pO_2 measured in mmHg. Measurements were made using a commercially available oxygen electrode (the 'Eppendorf' electrode). The values shown are the median of the median values for each patient. ND, not determined; pO_2, oxygen partial pressure.

Table adapted from REF 46.

1.4 HIF-1 (Hypoxia-inducible factor-1)

The transcription factor HIF-1 is a primary factor that mediates the cellular adaptations to hypoxia.

1.4.1 Regulation of HIF-1

HIF-1 is a heterodimer consisting of an oxygen-inducible alpha subunit and a constitutively expressed beta subunit (HIF-1α, HIF-1β). Under normoxic conditions, proline residues 402 and 564 within the HIF-1α oxygen dependent degradation domain (ODDD) are hydroxylated by prolyl hydroxylase domain containing enzymes (PHD). PHDs are effective oxygen sensors, as they have very high Km values for O_2 (slightly above the atmospheric oxygen concentrations), indicating that even small decreases in O_2 can attenuate their activities [45, 58]. Thus, proline 402/564 hydroxylation is an oxygen-dependent reaction. Hydroxylated HIF-1α forms hydrogen bonds with the von Hippel Lindau protein (pVHL) side chains. The pVHL associates with the proteins elongin C, elongin B, cullin-2, and Rbx1 to form the VCB-Cul2 E3 ligase complex, which tags HIF-1α with ubiquitin, leading to the subsequent degradation of HIF-1α by the 26S-proteasome[59, 60]. Thus under normoxic conditions, HIF-1α protein is unstable and has a short half-life (~5min) (Figure 1.1A) [60].

In addition to the regulation of HIF-1α stabilization, there is a second major mechanism that regulates HIF-1 activity. Under normoxic conditions, asparagine residue 803 within the HIF-1α C-terminal transactivation domain (CTAD) is hydroxylated by factor inhibiting HIF-1 (FIH-1). Like the PHDs, the asparaginyl hydroxylase FIH-1 also serves as an oxygen sensor. Hydroxylation of asparagine 803 prevents the association of HIF-1 with the transcriptional co-activator p300/CBP and thus inhibits the transcriptional activity of HIF-1 (Figure 1.1A) [45].

However, under hypoxic conditions, the activities of PHDs and FIH-1 are inhibited due to lack of oxygen. Under hypoxia, hydroxylation of proline 402 and 564 does not occur, and pVHL is unable to bind to HIF-1α. The latter therefore cannot be ubiquitinated and degraded. The stabilized HIF-1α protein translocates from the cytoplasm to the nucleus, where it associates with the HIF-1β subunit and forms the HIF-1 heterodimer. The inhibition of asparagine 803 hydroxylation under hypoxia enables the association of HIF-1 with transcriptional co-activator p300/CBP, leading to the activation of the *HIF-1α* gene and subsequent HIF-1 target gene transcription (Figure 1.1B) [60]. Besides the post-translational modifications discussed above, direct phosphorylation of HIF-1α has also been observed and it is likely that the mitogen-activated protein kinase (MAPK) pathway plays a role here [61]. This phosphorylation does not seem to affect HIF-1α stability but increases the transcriptional activity of HIF-1. It has been proposed that HIF-1β binds preferentially to the phosphorylated form of HIF-1α (Figure 1.1B) [60, 62].

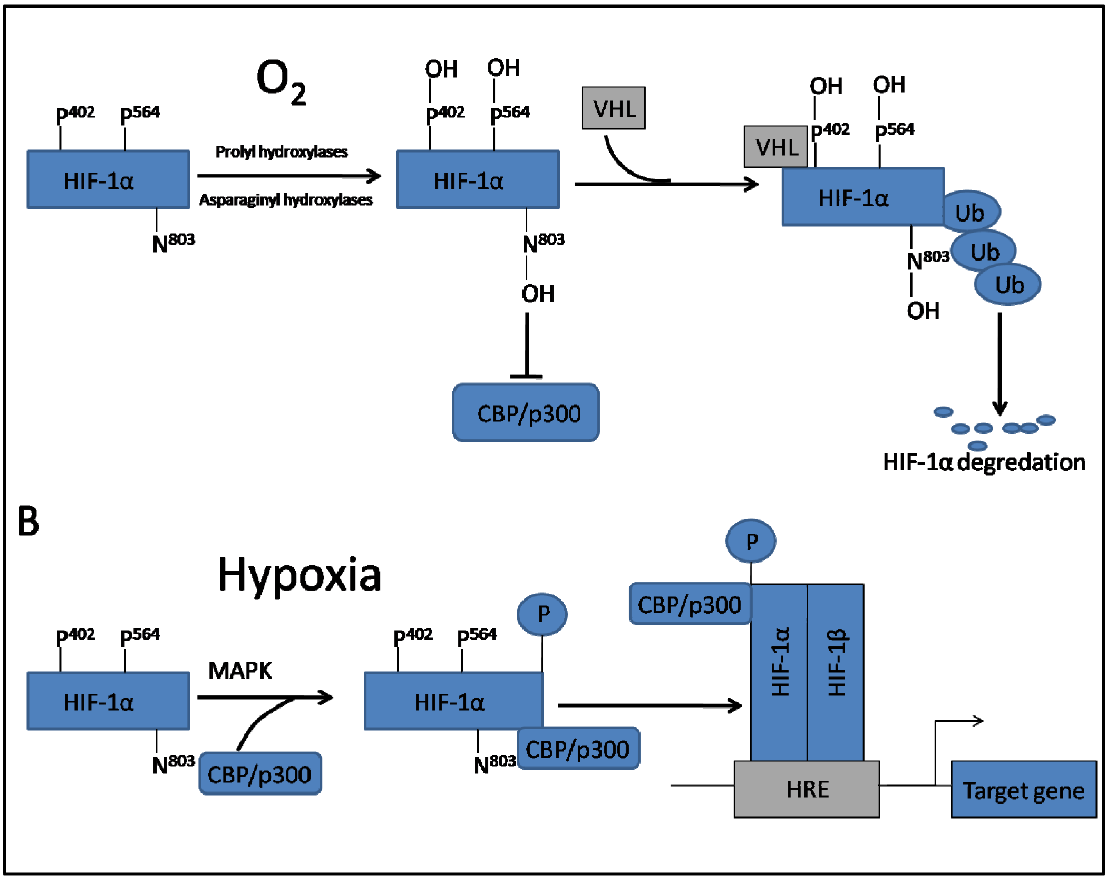

Figure 1.1 Oxygen-dependent regulation of HIF-1 stabilization and transactivation.

(A) In normoxia, hydroxylation of two proline residues of HIF-1α (P^{402} and P^{564}) leads to its binding to the E3 ubiquitin ligase VHL complex. The ligase complex tags HIF-1α with ubiquitin, leading to the subsequent degradation of HIF-1α by the proteasome. Meanwhile, hydroxylation of asparagine (N^{803}) blocks the recruitment of the transcriptional co-activator CBP/p300. **(B)** In hypoxia, the activities of hydroxylases are inhibited due to lack of oxygen, VHL is unable to bind to HIF-1α and HIF-1α is therefore stabilized. Stabilized HIF-1α protein translocates from the cytoplasm into the nucleus, where it associates with the HIF-1β subunit and forms the HIF-1 heterodimer. The inhibition of asparagine 803 hydroxylation under hypoxia enables the association of HIF-1 with the transcriptional co-activator p300/CBP, leading to the activation of the *HIF-1α* gene and subsequent HIF-1 target gene transcription.
Figure adapted from REF 60.

1.4.2 The target genes of HIF-1

Activation of HIF-1 results in the expression of targets whose enhancer and promoter regions contain HRE (hypoxia-responsive element) sites with the core DNA sequence 5'-ACGTG-3'[63].

To date, there are over 100 genes known to be up-regulated through HIF-1-mediated transcriptional activation. These include genes involved in erythropoiesis/iron metabolism, which can enhance the formation of erythrocytes and thereby the delivery of oxygen to tissues [63, 64]; genes involved in angiogenesis, such as the vascular endothelial cell growth factor (VEGF), that can recruit endothelial cells into hypoxic and avascular areas and can stimulate their proliferation [65-67]; and genes involved in glycolysis, resulting in increased expression of glycolytic enzymes and glucose transporters to generate more ATP to compensate for the low efficiency of the oxygen-independent glycolysis [68-70].

Moreover, HIF-1 can up-regulate target genes associated with cell proliferation/survival, such as insulin-like growth factor-2 (IGF2) and transforming growth factor-α (TGF-α) [71, 72]. Paradoxically, hypoxia can also lead to apoptosis in some circumstances: it has been shown that expression of HIF-1α and HIF-1β significantly correlates with apoptosis and pro-apoptotic factors, such as caspase-3, Fas, and Fas ligand [45, 60].

1.5 HIF-1 regulated Pro-protein Convertase Furin

The six classes of mammalian proteases are serine, metallo, cysteinyl, aspartyl, threonine, and glutamyl proteases [73]. Pro-protein convertases (PCs) are members of a family of nine Ca^{2+}-dependent serine proteases that process protein and peptide precursors as they move through the secretory pathway, and thus PCs are responsible for post-translational processing and activation of precursors of many proteins [74].

Seven of the PC family members cleave peptides at locations preceded by basic amino acids at the general consensus motif (Lys/Arg)-(X)n-(Lys/Arg)↓, where n=0, 2, 4 or 6 and X is any amino acid, and are called PC1/3, PC2, furin, PC4, PC5/6, PACE4 and PC7. The two other convertases, SKI-1/S1P and PCSK9, are implicated in cholesterol and/or fatty acid metabolism [74]. Within the PC family, members such as PC1, PC2, and PC4 are tissue-specific distributed, whereas furin, PACE-4, PC5/PC6, and PC7 are expressed in a broad range of tissues and cell lines [75].

The majority of proteins regulating the metastatic ability of tumour cells, such as adhesion molecules, growth factors, growth factor receptors, and metalloproteinases, are synthesized as inactive precursor proteins that are converted to their bioactive forms by PC family members [76]. Over-expression of PCs has been observed in lung, breast, colon, and head and neck carcinomas, and because of their role in the activation of matrix metalloproteinases (MMPs), PCs are thought to be linked to progression of a variety of cancers [75, 76].

Among the PC convertases, furin was the first identified and has been the most extensively studied. Furin is ubiquitously expressed and is mainly localized to the trans-Golgi network, though furin molecules are also known to cycle between the trans-Golgi network and the cell surface [77]. This enzyme is encoded by the *fur* gene, which stands for c-**f**es/fps proto-oncogene **u**pstream **r**egion. Furin activates precursors of many proteins including growth factors (*e.g.* transforming growth factor-β1, insulin-like growth factor-1, platelet-derived growth factor), serum proteins, receptors, viral-envelope glycoproteins, bacterial exotoxins, and various metalloproteinases. It acts at sites marked by the consensus Arg-Xaa-(Lys/Arg)-Arg↓ sequence [78]. It has also been reported that furin expression and activity are increased by hypoxia in a HIF-1-dependent manner [79]. Because of the critical role of furin in the activation of metalloproteinases (*e.g.* ADAMs) involved in the shedding of surface proteins, the hypothesis tested in the studies described in this thesis is that increased furin activity is an essential step in the mechanism of hypoxia-induced shedding of MICA and resistance of tumour cells to lysis by effector cells of the immune system.

1.6 Rationale and Hypothesis

Our laboratory's previous study showed that hypoxia can induce the shedding of membrane-bound MICA from the surface of DU-145 human prostate cancer cells, while at the same time, upon exposure to hypoxia, tumour cells acquire resistance to cytolysis by IL-2-activated peripheral blood lymphocytes (PBLs) [57]. Further study showed that, in the presence of an anti-MICA/MICB antibody which prevents MIC-NKG2D interactions, the sensitivity to the cytolytic activity of PBLs was significantly decreased in DU-145 cells pre-incubated in 20% O_2, while addition of anti-MICA/MICB antibody did not further decrease the sensitivity to PBL-mediated cytotoxicity in DU-145 cells pre-incubated in 0.5% O_2; thus it was concluded that hypoxia-induced MICA shedding can induce resistance of tumour cells to PBL-mediated lysis[57]. Identification of critical molecules involved in the pathway of hypoxia-induced membrane-bound MICA shedding is an important component of this thesis. Since Hypoxia Inducible Factor-1 (HIF-1) is a key mediator of cellular adaptations to hypoxia, the first hypothesis tested in the present studies is that **the hypoxia-induced shedding of MICA from the cancer cell surface is dependent on HIF-1 expression and activity** (Figure 1.2).

A previous study revealed that the expression and activity of the pro-protein convertase furin are increased by hypoxia in a HIF-1-dependent manner [79]. Since furin is a key player in the activation of metalloproteinases involved in the shedding of surface proteins, the second hypothesis tested here is that **furin expression and activity in**

cancer cells are increased by hypoxia and are required for the hypoxia-induced shedding of MICA from cancer cell surface (Figure 1.2).

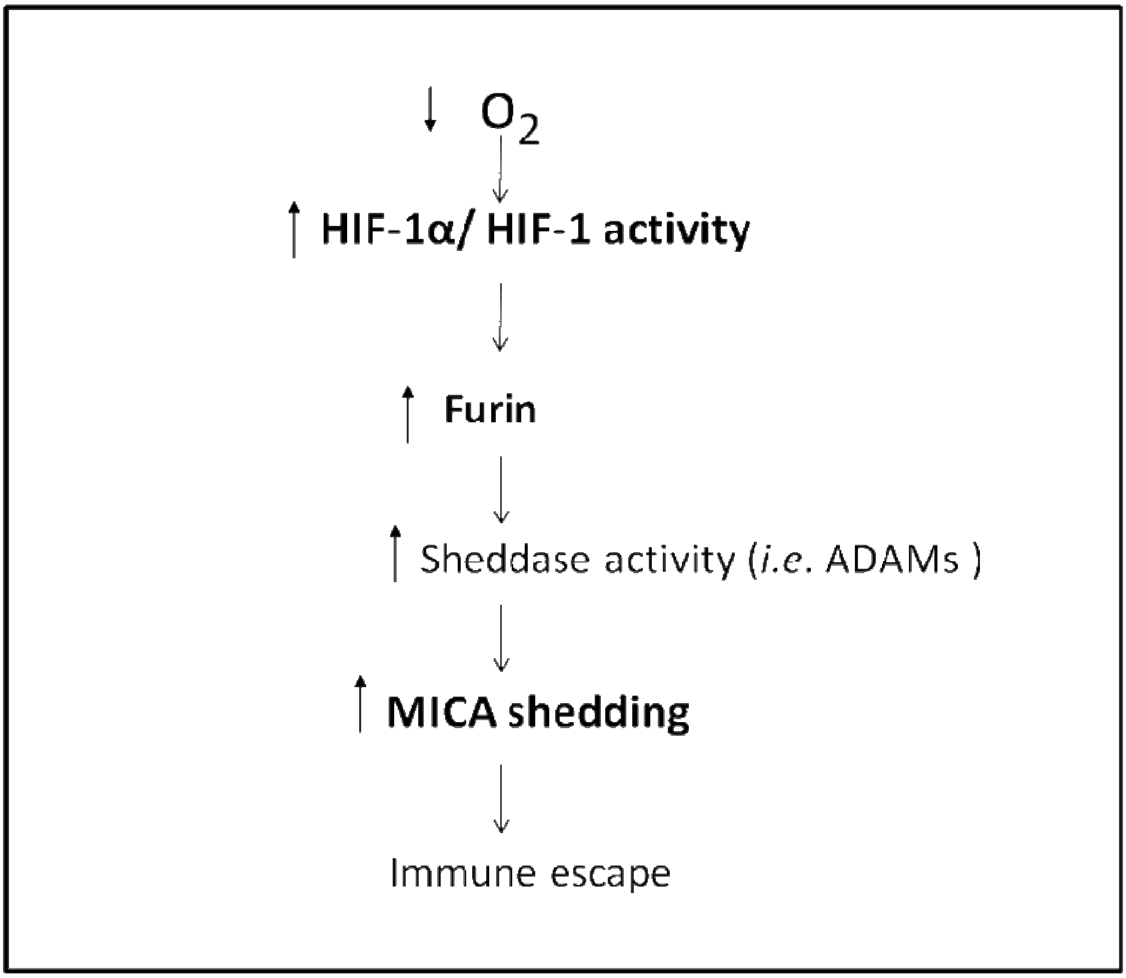

Figure1.2 Proposed mechanism of hypoxia-mediated immune escape

1.7 Objectives

1. To determine whether the shedding of MICA from cancer cell surface requires the expression of hypoxia inducible factor-1 (HIF-1).

2. To determine whether furin expression/activity is increased during hypoxia-induced shedding of MICA from cancer cell surface.

Chapter 2

Materials and Methods

2.1 Cell culture

Human MDA-MB-231 breast carcinoma cells and human DU-145 prostatic carcinoma cells were obtained from the American Type Culture Collection (Manassas, VA, USA). Cells were maintained in monolayer culture in RPMI 1640 medium supplemented with 5% FBS (Invitrogen, Burlington, ON, Canada). Cells were cultured in a standard Thermo Forma CO_2 incubator (5% CO_2 in air at 37^{o}C).

MDA-MB-231 cells were initially isolated from a pleural effusion obtained from a 51-year-old patient. They are invasive and metastatic, are estrogen receptor negative, and do not express wild-type p53 tumour suppressor protein [80].

DU-145 cells were initially derived from a human prostate adenocarcinoma metastatic to the brain. They are not detectably hormone-sensitive and do not express prostate-specific antigen [81, 82].

2.2 Exposure to hypoxic conditions

To establish hypoxic conditions, cells were placed in airtight plastic chambers that were flushed with a 5% CO_2/ 95% N_2 gas mixture (BOC, Kingston, ON, Canada). Different oxygen tensions within these chambers were maintained by Pro-Ox Model 110 O_2 regulators (Biospherix, Redfield, NY, USA). Fresh medium was always replaced immediately prior to incubation in 0.5% O_2 or 20% O_2.

2.3 Small interfering RNA (siRNA) transfection

A transfection reagent, siPORT™ NeoFX™ (Ambion Inc., Austin, TX, USA) was used according to the manufacturer's instructions to introduce siRNA into cells.

For siRNA uptake optimization, Silencer FAM-labelled GAPDH siRNA (Ambion) was introduced into cells and flow cytometry was used to determine the fluorescent signal of the cells that took up the siRNA (cells exhibiting fluorescence).

Knockdown of HIF-1α expression was achieved using Silencer validated siRNA targeted against exon 5 of the human HIF-1α gene (ID #42840; Ambion). Silencer Negative Control siRNA #1 (Ambion), Silencer Negative Control siRNA #2 (Ambion), and AllStars Negative Control siRNA (Qiagen, Mississauga, ON, Canada) were used as negative controls to assess for any non-specific effects of transfection.

2.4 Western blot analysis

Following incubation under various conditions, cells were removed from the hypoxia chambers and frozen immediately by rapidly discarding the media and placing the culture plates in a liquid nitrogen bath. Cells were lysed on ice using 80-100 µl HIF-1 lysis buffer [100 mM NaCl, 20 mM Tris HCl pH 7.6, 5 mM $MgCl_2$, 0.5% Igepal CA630, Protease Inhibitor Cocktail(Roche Diagnostics, Laval, QC, Canada)] for a 6-cm plate. Lysates were briefly sonicated (one 10-sec. burst at 50 Hz) then centrifuged (5 minutes at 14,000 x g at 4^{o}C). Determination of protein content was performed using a modified Lowry assay (Bio-Rad DC Protein Assay, Bio-Rad Laboratories, Mississauga, ON, Canada). Lysates were stored at -80^{o}C until use.

Protein samples of 15-100 μg were resolved on 6-10% SDS-polyacrylamide gels and transferred onto Immobilon-P membranes (Millipore Corporation, Bedford, MA, USA) using a wet transfer apparatus. Membranes were incubated in TBS (140 mM NaCl, 50 mM Tris HCl pH 7.2) containing 5% milk powder (w/v) in a hybridization incubator for 1 h at room temperature in order to block non-specific binding.

After blocking, the membranes were incubated with primary antibody in TBS/0.5% milk overnight at 4^{o}C. Primary antibodies used included HIF-1α antibody, 1:250 (BD Transduction Laboratories, Oakville, ON, Canada); furin antibody (MON-152; Axxora, San Diego, CA, USA); α-tubulin antibody, 1:20000 (Sigma-Aldrich Canada Ltd.); β-actin antibody, 1:5000 (Sigma-Aldrich Canada Ltd.). All of the primary antibodies were monoclonal antibodies produced in mouse.

The membranes were washed in TBS containing 0.1% Tween 20 (6 × 5 min) and then incubated for 1 h at room temperature (RT) with secondary antibody in TBS/0.5% milk. The secondary antibody used was horseradish peroxidase-conjugated goat anti-mouse (1:5000; Biorad). Membranes were then washed in TBS containing 0.1% Tween 20 (6 ×

5 min). Secondary antibodies were detected by enhanced chemiluminescence (Amersham Biosciences, Baie D'Urfe, QC, Canada) and exposure to Kodak X-Omat Blue Film.

2.5 Flow Cytometry

Flow cytometry was used to monitor siRNA uptake efficiency and to measure membrane-bound MICA expression.

Silencer FAM-labelled GAPDH siRNA uptake efficiency was analyzed with a Beckman Coulter EPICS Altra HSS flow cytometer (Beckman-Coulter). Excitation was performed by an argon laser at a wavelength of 488 nm, the emitted fluorescence was collected at 525 ± 20 nm, and at least 10,000 events per sample were analyzed.

Surface expression of MICA on tumour cells was analyzed with the same flow cytometer. In preparation for flow cytometry, tumour cells were plated and allowed to reach 80% confluence. Cells were then incubated in a standard CO_2 incubator (20% O_2) or were placed in 0.5% O_2 for 24 h. Cells were then harvested with 5 mM EDTA, washed twice with washing buffer (PBS containing 2% FBS), incubated with mouse anti-human MICA/MICB monoclonal antibody, 1:10 (Santa Cruz Biotechnology, CA, USA) or mouse anti-human MICA monoclonal antibody, 1:10 (Santa Cruz Biotechnology) for 1 h on ice, washed three times with washing buffer, incubated with FITC-conjugated goat anti-mouse antibody, 1:10 (Dako, Mississauga, ON, Canada) for 1 h and then analyzed by flow cytometry. Excitation was performed by an argon laser at a wavelength of 488 nm, the emitted fluorescence was collected at 525 ± 20 nm, and at least 10,000 events per sample were analyzed.

2.6 Determination of mRNA by real-time PCR

Total RNA was isolated using High Pure RNA Isolation Kit (Qiagen) according to the manufacturer's protocol. One μg of total RNA sample was reverse-transcribed with Transcriptor Reverse Transcriptase (Roche, Mississauga, ON, Canda) using a random hexamer (Cortex, Kingston, ON, Canada). Real-time PCR was conducted by an Corbett Research Rotor-Gene 3000 (Corbett Robotics Inc, San Francisco, USA), using SYBR Green PCR Master Mix (Roche) and gene-specific primers as follows: Furin sense 5'-GGCATTGTGGTCTCCATT-3' and antisense 5'- ATCTGTCACCTCGCCATC-3'; 18S sense 5'-GCCCGAAGCGTTTACTTTGA-3' and antisense 5'-TCCATTATTCCTAGCTGCGGTA-3'. Real-time PCR conditions for furin were 95°C for 5 min, followed by 45 cycles of 95°C for 10 sec, 61°C for 20 sec and 72°C for 30 sec; for 18S were 95°C for 3 min, followed by 35 cycles of 95°C for 15 sec, 62°C for 20 sec and 72°C for 20 sec. SYBR Green dye intensity was analyzed using Rotor-Gene 6 software (Corbett). The mRNA level of each gene was normalized against 18S mRNA levels. The specific transcripts were confirmed by melting curve analysis at the end of each PCR cycle, and the specificity of the PCR was further verified by subjecting the amplification products to agarose gel electrophoresis [83].

2.7 Pro-Protein Convertase Activity Assay

Tumour cells (1.5×10^4 or 2.0×10^4) were plated in 96-well plates and incubated in a standard CO_2 incubator (20% O_2) overnight. Fresh medium was replaced and cells were incubated in 0.5% O_2 or 20% O_2 for 24 h. Adherent cells were then assayed in the presence of 0.25% Triton X-100 (as a permeabilizing agent) and the fluorogenic substrate Boc-RVRR-AMC (100 μM) (Bachem Americas, Inc. Torrance, CA, USA) at 37^{o}C for 5 h. Boc-RVRR-AMC is a substrate for furin (Km=50 μM), and other pro-protein convertases, such as PC2 (Km=40 μM), PC1/3 (Km=66 μM). Upon cleavage, AMC (7-amino-4-methylcoumarin) is liberated, and fluorescence was measured at 380-nm excitation and 460-nm emission wavelengths. The data were normalized to cell density by parallel staining of another 96-well plate with crystal violet [84-86]. To pool the data from five independent experiments, data were then normalized to results obtained from cells incubated under standard conditions (20% O_2) within each experiment.

2.8 Calculations and statistical analysis

For flow cytometric analysis, at least 10,000 cells per sample were analyzed. The level of membrane-bound MICA expression was presented as the median fluorescence intensity of the cells. The relative change in membrane-bound MICA expression of cells in 0.5% O_2 versus 20% O_2 was determined by subtracting the median fluorescence intensity of cells incubated in 20% O_2 from that of cells incubated in 0.5% O_2, and then divided by the median fluorescence intensity of cells incubated in 20% O_2.

To quantify the knockdown efficiency of HIF-1α from Western blot results (showing the level of HIF-1α expression), densitometric analysis was performed using Scion Image software (Scion Corporation, Frederick, Maryland, USA). To pool data from independent experiments, data were normalized to results obtained from untransfected cells incubated under hypoxic conditions (0.5% O_2) within each experiment.

For the furin activity assay, fluorescence readings were normalized to cell density by parallel staining of another 96-well plate with crystal violet. To pool the data from independent experiments, data were normalized to results obtained from cells incubated under standard conditions (20% O_2) within each experiment.

In the present study, data are reported as the mean ± the standard error of the mean (SEM). Statistical analyses were performed using GraphPad Prism software version 4.0 (GraphPad Software, Inc., San Diego, CA, US). When only two groups were compared, statistical significance was determined by a paired, two-tailed t-test. One-sample t-tests were used when groups were compared against normalized control values. When more than two groups were compared, statistical significance was determined by one-way ANOVA followed by Bonferroni Comparison test. All statistical tests were two-sided and differences were considered to be statistically significant at $P < 0.05$. 95% confidence intervals (CI) are included where appropriate.

Chapter 3

Results

3.1 Optimization of siRNA uptake

To achieve good knockdown efficiency for HIF-1α, siRNA uptake optimization experiments were performed using human DU-145 prostate cancer cells and MDA-MB-231 breast cancer cells.

To determine the appropriate concentration of siRNA and transfection reagent NeoFX to be used in DU-145 cells, 10 nM, 25 nM, 40 nM or 50 nM Silencer FAM-labelled GAPDH siRNA together with 2.5 µl, 5 µl, 10 µl or 15µl of NeoFX were added to wells of a 6-well plate containing 1.2×10^5 DU-145 cells/well. After a 48-h incubation in a standard CO_2 incubator, cells were subjected to flow cytometric ayalysis to measure the siRNA uptake efficiency.

Results showed uptake of siRNA in 66.5% cells using 40 nM siRNA plus 10 µl NeoFX, which is close to the maximum uptake efficiency of 66.9% obtained with 40 nM siRNA plus 15 µl NeoFX (Table 3.1). Thus, a transfection mix consisting of 40 nM siRNA plus 10 µl NeoFX was used for further study using DU-145 cells.

Since the purpose of this experiment was only to determine the optimal transfection conditions for DU-145 cells, it was not repeated.

Similar optimization experiments were previously performed in the laboratory with MDA-MB-231 cells, and uptake of siRNA in 75-85% of these cells was observed using 25 nM siRNA plus 10 µl NeoFX (R. Sullivan, unpublished observations).

3.2 HIF-1α knockdown

To knockdown HIF-1α expression, siRNA targeting HIF-1α was introduced into MDA-MB-231 cells and DU-145 cells. Cells were then incubated for 24h under standard conditions followed by a 24-h incubation in either a 0.5% O_2 hypoxic chamber or a standard CO_2 incubator (20% O_2). Cell lysates were then subjected to Western blot analysis to measure the efficiency of HIF-1α knockdown.

The molecular weight of HIF-1α protein is 120 kD and a slightly higher molecular weight band observed represents the phosphorylated form of HIF-1α protein. The molecular weight of α-tubulin is approximately 50 kD.

Densitometric analysis revealed that transfection with HIF-1α siRNA decreased HIF-1α protein levels in DU-145 cells by approximately 30% (Figure 3.1) and by about 80% in MDA-MB-231 cells compared with controls (Figure 3.2).

To determine the persistence of HIF-1α knockdown in MDA-MB-231 cells, a time-course study was performed and results showed that more than 70% knockdown efficiency was maintained 96 h following the transfection with siRNA (Figure 3.3).

Table 3.1 siRNA uptake optimization in DU-145 cells

NeoFX (µl)	0	2.5	5	5	5	10	10	**10**	15	15
FAM™ labelled GAPDH siRNA(nM)	0	10	10	25	50	10	25	**40**	25	40
Percentage of cells exhibiting fluorescence	2.1	19.5	34.6	37.5	35.7	56.1	50.1	**68.6**	53.3	69

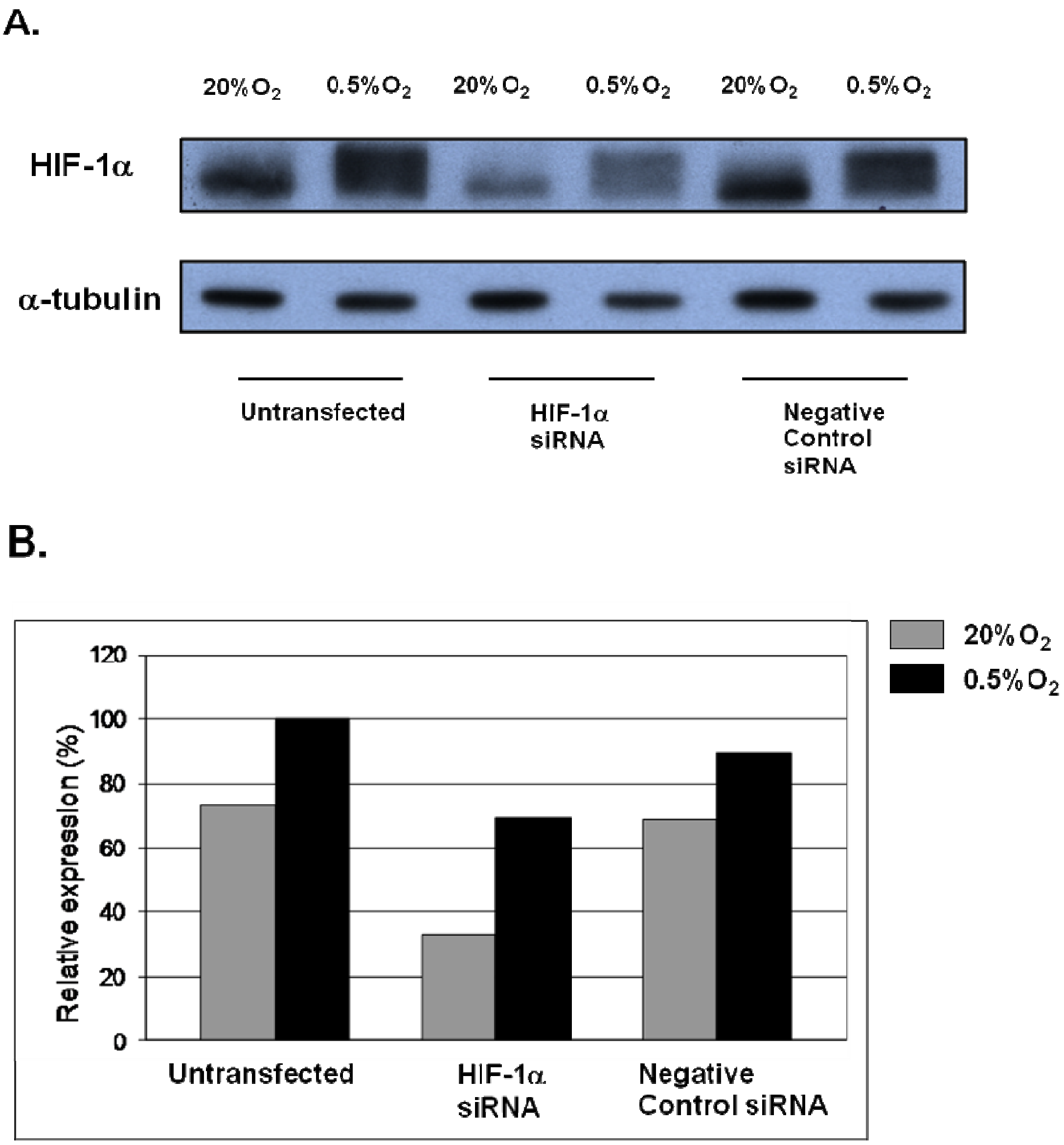

Figure 3.1 HIF-1α knockdown optimization using siRNA in human DU-145 prostate cancer cells. DU-145 cells were plated at a density of 1.2×10^5 cells/well in a 6-well plate. 40 nM HIF-1α siRNA or negative control siRNA was introduced into cells by 10 µl NeoFX. Cells were then incubated for 24 h under standard conditions followed by 24 h incubation in either 0.5% O_2 or 20% O_2. **(A)** Cell lysates were subjected to Western blot analysis using anti-HIF-1α or anti-α-tubulin monoclonal antibody. **(B)** Results of densitometric analysis of blot shown in (A).

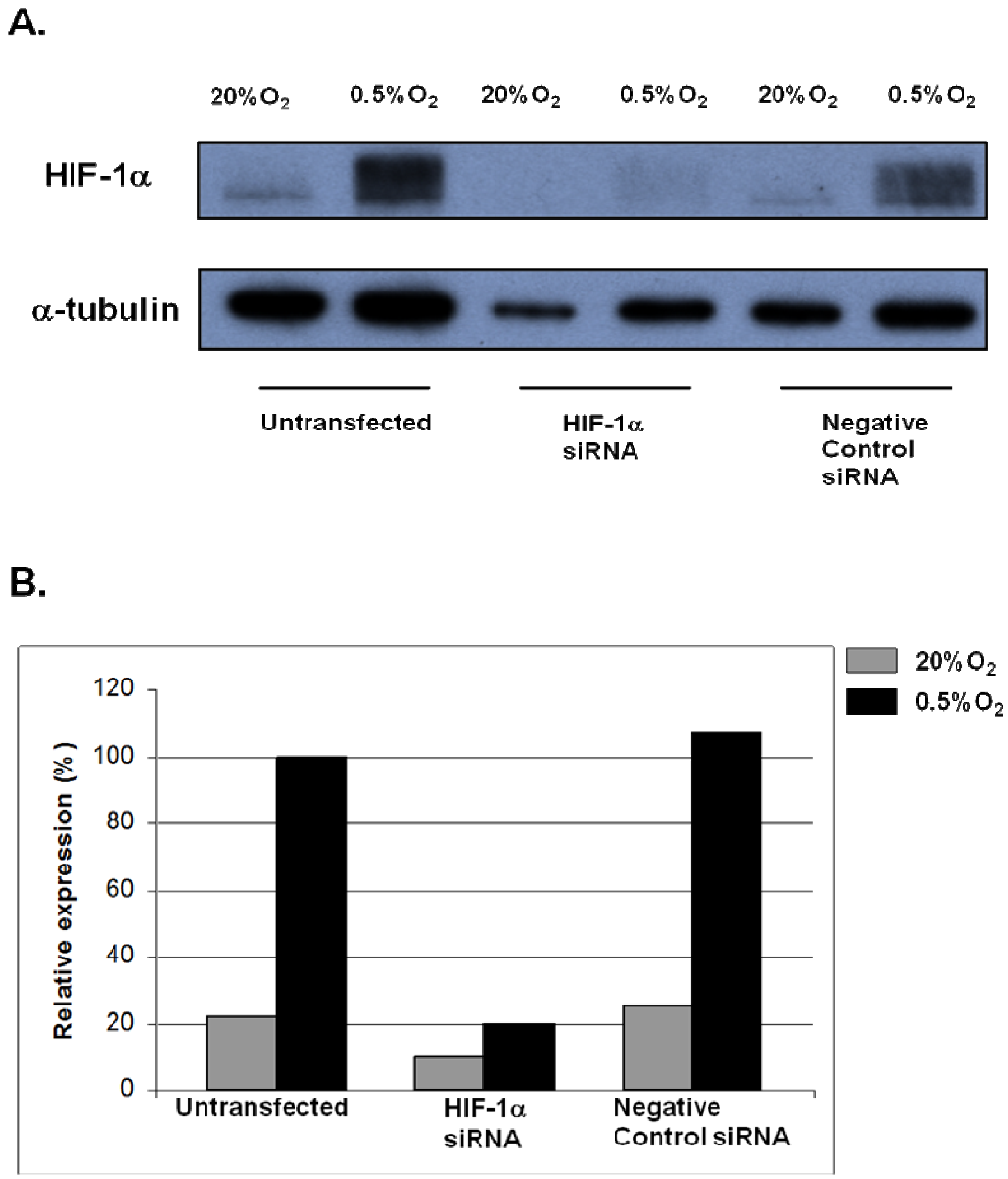

Figure 3.2 HIF-1α knockdown optimization using siRNA in human MDA-MB-231 breast cancer cells. MDA-MB-231 cells were plated at a density of 6.5×10^4 cell/well in a 6-well plate. 25 nM HIF-1α siRNA or negative control siRNA was introduced into the cells using 10 µl NeoFX. Cells were then incubated for 24h under standard conditions followed by a 24-h incubation in either 0.5% O_2 or 20% O_2. **(A)** Cell lysates were then subjected to Western blot analysis using anti-HIF-1α or anti-α-tubulin monoclonal antibody. **(B)** Results of densitometric analysis of blot shown in (A).

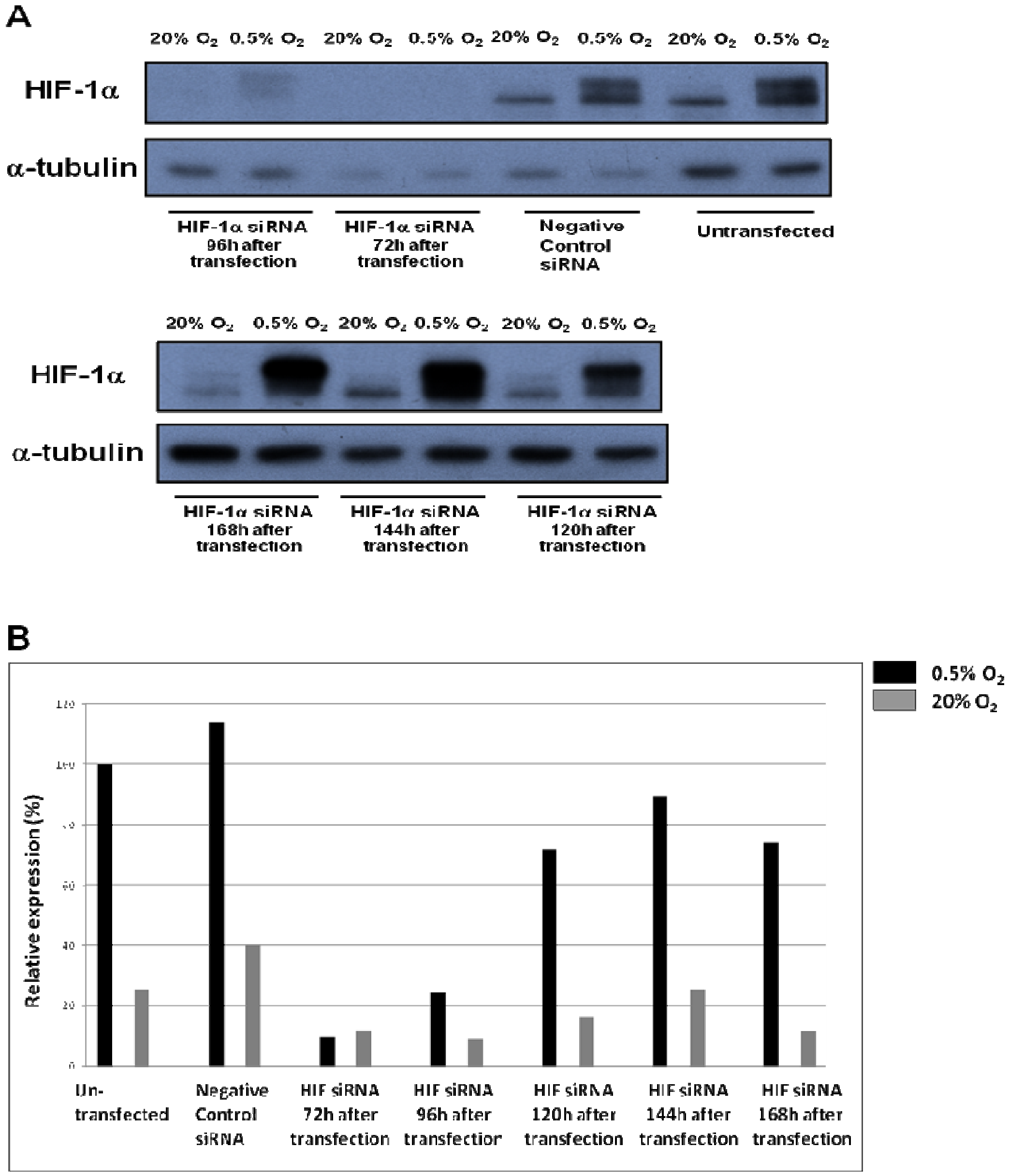

Figure 3.3 Time-course of HIF-1α knockdown in MDA-MB-231 cells. Cells were transfected with HIF-1α siRNA or negative control siRNA for 24 h. Medium containing siRNA was then replaced with fresh culture medium. Cells were then incubated for 24 h, 48 h, 72 h, 96 h, or 120 h under standard conditions followed by a 24-h incubation in either 0.5% O_2 or 20% O_2. **(A)** Cell lysates were then subjected to Western blot analysis using anti-HIF-1α or anti-α-tubulin monoclonal antibody. **(B)** Results of densitometric analysis of blot shown in (A). This experiment was performed once.

3.3 Shedding of membrane-bound MICA under hypoxia

3.3.1 Shedding of membrane-bound MICA after 24-h of hypoxia in 0.5% O_2

To confirm that hypoxia induces the shedding of MICA in DU-145 prostate cancer cells, the latter were incubated under hypoxia (0.5% O_2) or standard conditions (20% O_2) for 24 h. Results of flow cytometry using an antibody that recognizes both MICA and MICB revealed that the levels of membrane-bound MIC were 20% lower in DU-145 cells incubated for 24 h in 0.5% O_2 versus 20% O_2 (Figure 3.4).

To determine whether a similar hypoxia-mediated shedding of membrane-bound MIC occurs in human MDA-MB-231 breast cancer cells, these cells were incubated in hypoxia (0.5% O_2) or standard conditions (20% O_2) for 24 h. Results of flow cytometry using an antibody that specifically recognizes MICA revealed a mean 40% decrease in the levels of membrane-bound MICA on MDA-MB-231 cell surface after a 24-h incubation under 0.5% O_2 (Figure 3.5).

Since MDA-MB-231 cells exhibited a substantially more robust response to hypoxia (in terms of hypoxia-induced shedding of MIC) than DU-145 cells, the former cells were used in subsequent experiments.

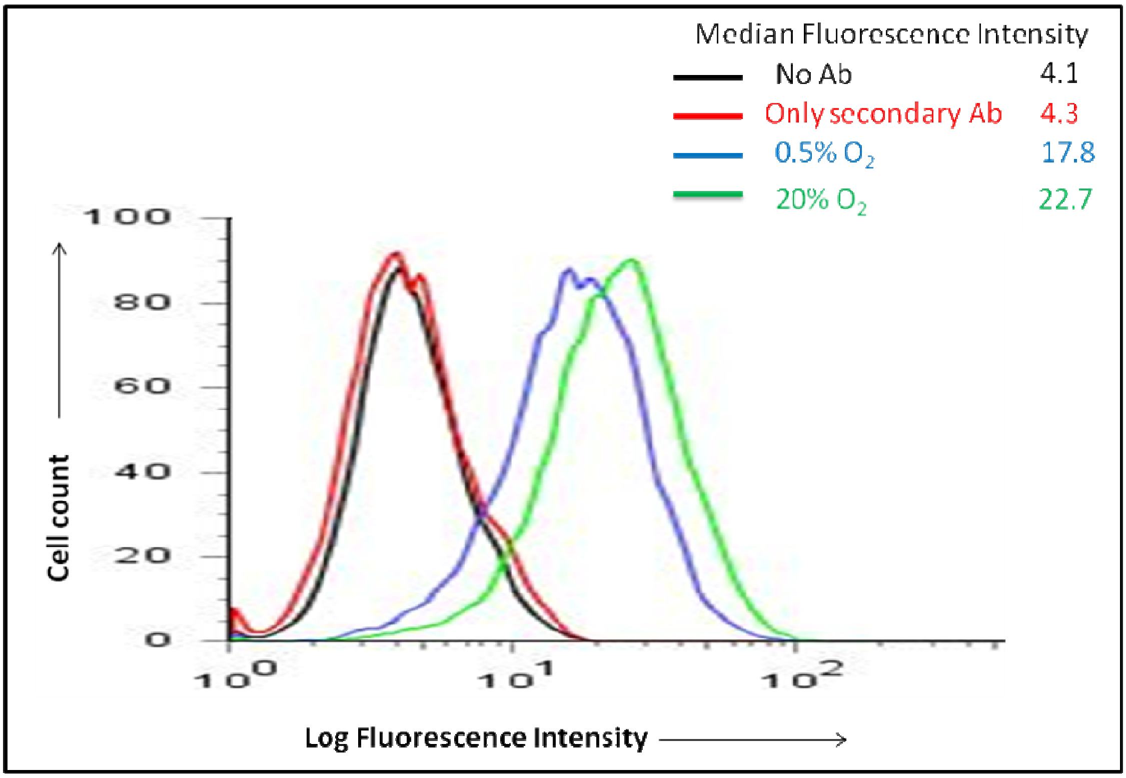

Figure 3.4 Hypoxia-induced mMIC shedding from DU-145 cell surface. Cells were plated at a density of 4.5×10^{5} cells/60-mm dish and incubated in a standard CO_2 incubator overnight. Cells were then incubated in 0.5% O_2 or 20% O_2 for 24 h. They were harvested and analyzed by flow cytometry using anti-MICA/B antibody. Results revealed an approximately 20% decrease in the levels of membrane-bound MIC on DU-145 cells incubated in 0.5% O_2 compared to 20% O_2.This experiment was repeated at least three times. Data shown here are results of a single experiment.

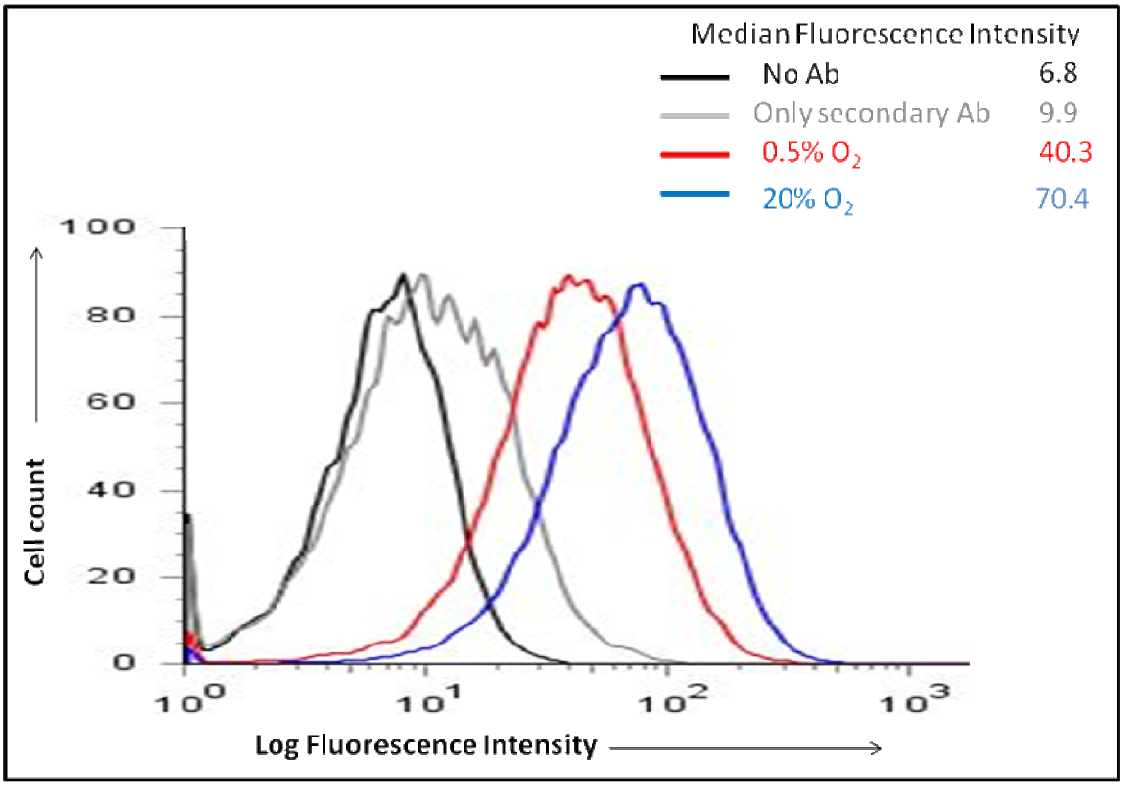

Figure 3.5 Hypoxia-induced mMICA shedding from MDA-MB-231 cell surface. Cells were plated at a density of 3.1×10^5 cell/60-mm dish and incubated in a standard CO_2 incubator overnight. Cells were then incubated in 0.5% O_2 or 20% O_2 for 24 h and subsequently subjected to flow cytometric analysis using anti-MICA antibody to determine the level of surface MICA. Results revealed a mean 40% ($P < 0.01$, n=5) decrease in the levels of membrane-bound MICA after incubation in hypoxia. Data shown are from a representative of five independent experiments.

3.3.2 Time-course of membrane-bound MICA shedding from the tumour cell surface

To determine the optimal time point to analyze the shedding of mMICA from the tumour cell surface (*i.e.* when maximal shedding has occurred), a time-course study was conducted. MDA-MB-231 cells were incubated for 3.5 h, 12 h, or 24 h under 0.5% O_2 or 20% O_2. Results of flow cytometry using an antibody that specifically recognizes MICA revealed the shedding reached its maximum by 24 h of incubation at 0.5% O_2 (Figure 3.6).

As the goal of this experiment was to determine the optimal exposure to hypoxia for subsequent experiments, it was only conducted once. For the purpose of convenience, 24-h exposure to hypoxia was used in subsequent experiments.

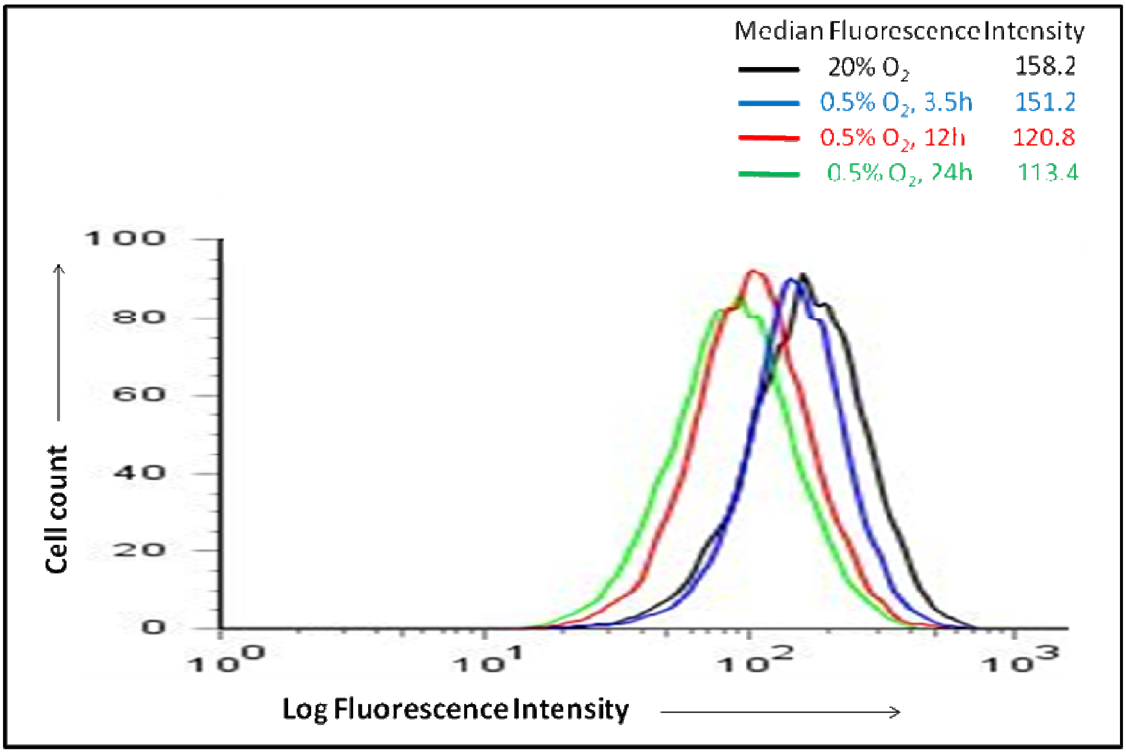

Figure 3.6 Time-course of hypoxia-induced mMICA shedding from the surface of MDA-MB-231 cells. Cells were plated at a density of 3.1×10^5 cells/60-mm dish and incubated in a standard CO2 incubator overnight. After a 3.5-h, 12-h, or 24-h incubation in 0.5% O_2 or 20% O_2, cells were subjected to flow cytometric analysis using anti-MICA antibody to determine the level of surface MICA (n=1). Because incubations at 20% O_2 for 3.5 h and 12 h yielded similar level of surface MICA, for simplicity's sake, only results of control cells incubated for 24 h in 20% O_2 are shown.

3.4 MICA shedding vs. HIF-1α knockdown

To test the hypothesis that the shedding of MICA from the tumour cell surface is HIF-1 dependent, HIF-1α expression was knocked down using HIF-1α siRNA. The expectation was that inhibition of HIF-1 activity through the knockdown of HIF-1α expression would block the hypoxia-mediated shedding of MICA from the surface of tumour cells.

MICA is a stress-inducible molecule and manipulation of cells during transfection is likely a stressful process. Since in the present studies, more than 70% knockdown efficiency was still maintained 96 h following transfection (Figure 3.3), MDA-MB-231 cells were transfected with HIF-1α siRNA or negative control siRNA for 24 h and then allowed to recover for 48 h under standard culture conditions. This recovery was followed by a 24-h incubation in either 0.5% O_2 or standard conditions (20% O_2). Cells were then subjected to flow cytometric analysis of surface MICA. Results revealed that the levels of membrane-bound MICA decreased on the surface of MDA-MB-231 cells after a 24-h incubation in 0.5% O_2 [relative change: mean ± SEM: -41.2 ± 3.3%; 95% CI: (-49.7%, -32.7%); $P < 0.0001$], but this decrease was prevented when the expression of HIF-1α was knocked down using siRNA [relative change: mean ± SEM: -12.1 ± 8.4%; 95% CI: (-33.8%, 9.6%); $P = 0.21$]. The decrease in surface MICA levels still occurred in cells transfected with negative control siRNA [relative change: mean ± SEM: -39.9 ± 5.6%; 95% CI: (-53.5%, -26.2%); $P < 0.0005$] (Figure 3.7). Parallel plates were subjected to Western blot analysis using HIF-1α monoclonal antibody to verify the knockdown of HIF-1α expression (Figure 3.8).

A

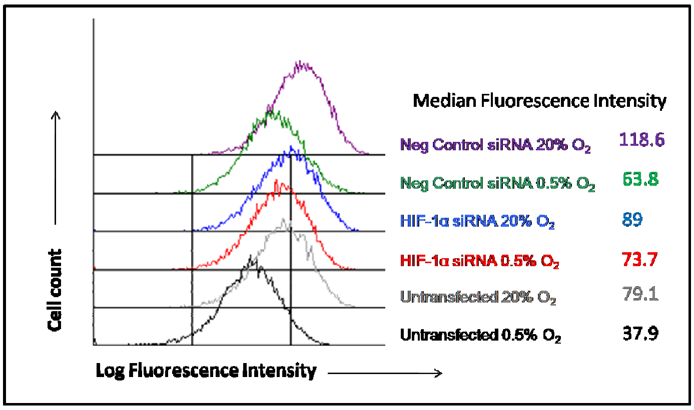

B

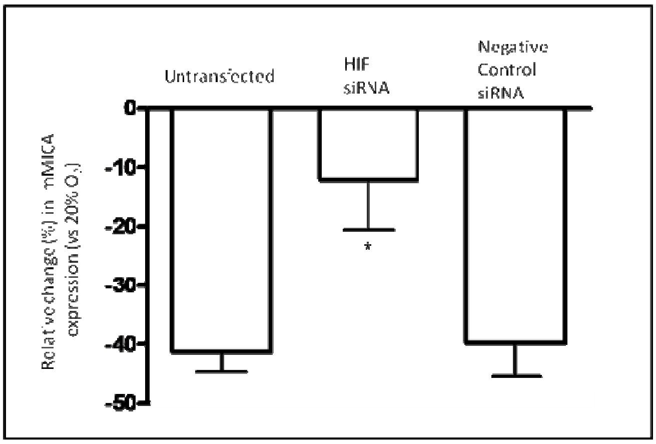

Figure 3.7 Hypoxia-induced mMICA shedding from MDA-MB-231 cell surface was blocked by the knockdown of HIF-1α. MDA-MB-231 cells were plated at a density of 6.5×10^4 cells/well in a 6-well tissue culture plate. 25 nM HIF-1α siRNA or negative control siRNA was introduced into the cells using 10 µl NeoFX and cells were incubated for 24 h under standard conditions. Medium containing siRNA was then replaced with fresh culture medium. Cells were then incubated for another 48 h under standard conditions (to allow for recovery) followed by a 24-h incubation in either 0.5% O_2 or 20% O_2. Cells were subjected to flow cytometric analysis using anti-MICA antibody to determine the level of surface MICA. (A) Flow cytometry results of membrane-bound MICA level from a representative experiment of five experiments. (B) Pooled results of flow cytometric analyses from five independent experiments. Data are presented as the relative change in membrane-bound MICA expression of cells in 0.5% O_2 versus 20% O_2 (mean ± SEM). Statistically significant differences of the change in membrane-bound MICA (mMICA) relative to the untransfected control are indicated (*$P<0.05$).

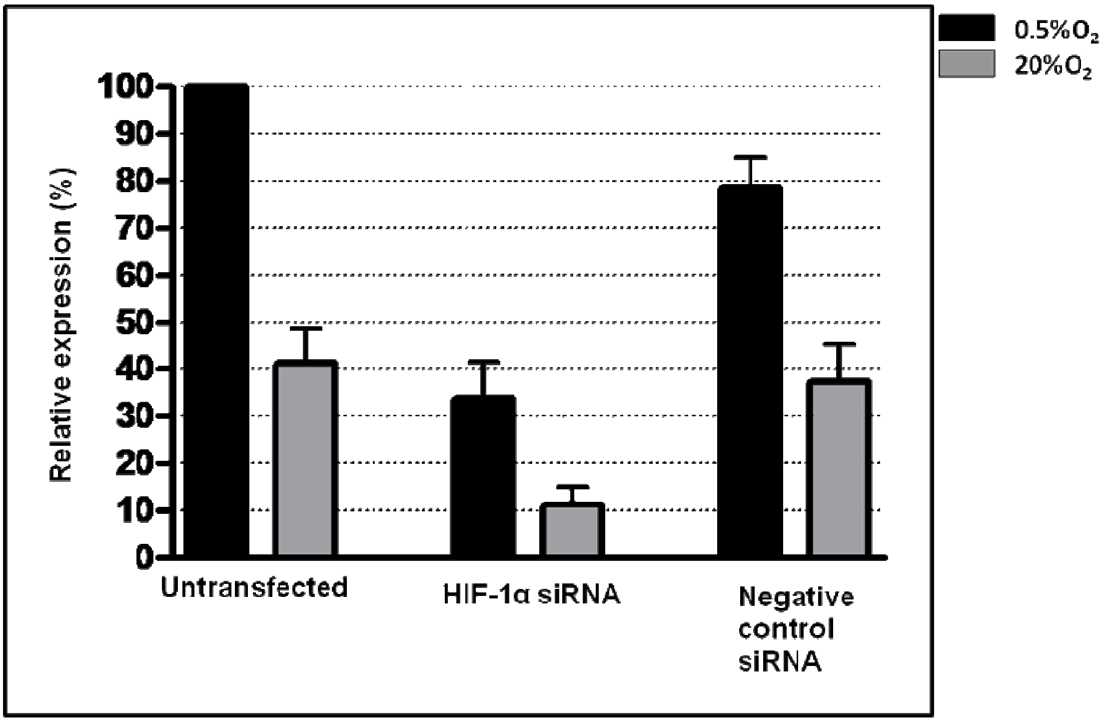

Figure 3.8 Confirmation of HIF-1α knockdown. MDA-MB-231 cells were plated at a density of 6.5×10^4 cells/well in a 6-well plate. 25 nM HIF-1α siRNA or negative control siRNA was introduced into cells using 10 µl NeoFX and cells were incubated for 24h under standard conditions. Medium containing siRNA was then replaced with fresh culture medium. Cells were incubated for another 48 h under standard conditions (to allow for recovery) followed by a 24-h incubation in either 0.5% O_2 or20% O_2. Cells were subjected to Western blot analysis using anti-HIF-1α monoclonal antibody to verify knockdown efficiency. Figure shows pooled results of densitometric analyses from eight independent experiments. Data were normalized to untransfected cells grown under hypoxia within each experiment, and are presented as the mean ± SEM (n=8).

3.5 Furin expression and activity under hypoxia

To test the hypothesis that furin expression and activity are increased by hypoxia, MDA-MB-231 cells were incubated under hypoxia (0.5% O_2) or standard conditions (20% O_2) for 24 h.

To determine the levels of furin mRNA, total RNA was isolated from the cells and then reverse-transcribed and subjected to real-time quantitative PCR (qPCR) analysis. Results of qPCR revealed that there was no increase in furin mRNA levels in cells incubated for 24 h in hypoxia (Figure 3.9A).

To study the level of furin protein expression, cells were subjected to Western blot analysis. The molecular weight of Furin protein is approximately 100 kD. The molecular weight of β-actin is 43 kD. Results of Western blot analysis revealed that there was no significant increase in furin protein levels in cells incubated for 24 h in hypoxia (Figure 3.9B).

To study furin activity following incubation in hypoxia, cells were subjected to a pro-protein convertases activity assay (see Material and Methods). Results of the assay revealed that pro-protein convertase activity was significantly increased after 24 h of hypoxia [Figure 3.10, mean ± SEM: 119.8 ± 11.3%, 95% CI: (88.43, 151.2), p=0.0005, n=5 for cells plated at a density of 1.5×10^4 cells/well; mean ± SEM: 125.6 ± 16.6%, 95% CI: (79.5, 171.8), p=0.0017, n=5 for cells plated at a density of 2.0×10^4 cells/well]. Similar results were also obtained using DU-145 cells (Data not shown).

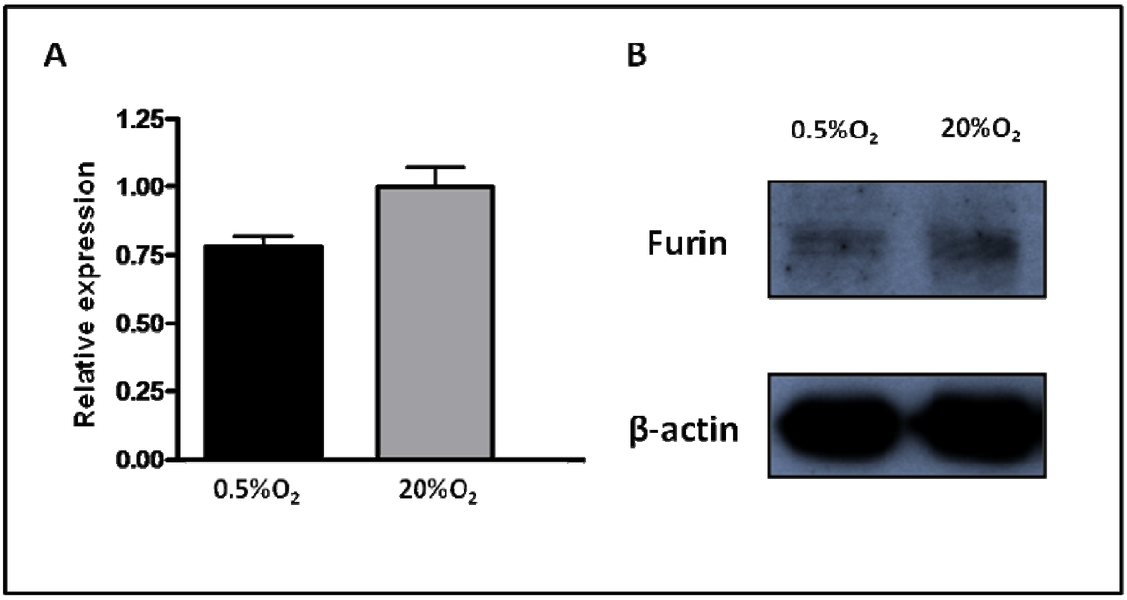

Figure 3.9 Furin expression after 24 h of hypoxia in MDA-MB-231 cells. Cells were plated at a density of 3.1×10^5 cells/60-mm dish and incubated in a standard CO_2 incubator overnight. Cells were then incubated in 0.5% O_2 or 20% O_2 for 24 h. (A) Total RNA was isolated from the cells and then reverse-transcribed. The level of mRNA expression was compared by real-time quantitative PCR. Data are the mean ± SEM of a representative experiment performed in triplicate. This experiment was performed twice. (B) Cells lysates were subjected to Western blot analysis using anti-furin or anti-β-actin monoclonal antibody. This experiment was performed once.

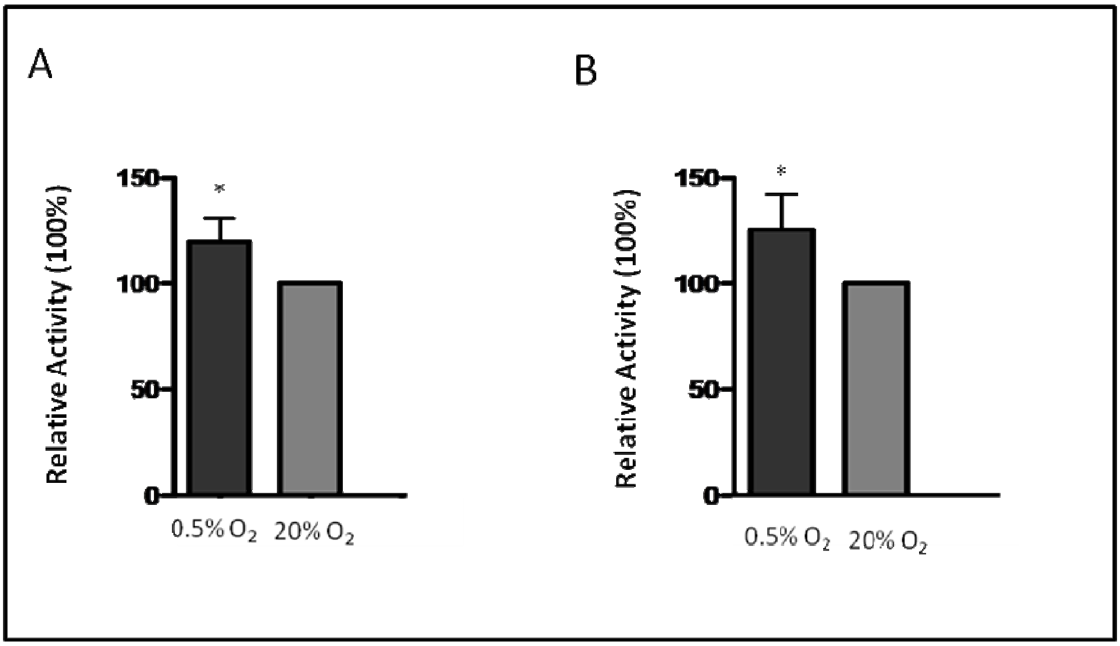

Figure 3.10 Pro-protein convertase activity following incubation in hypoxia. MDA-MB-231 cells were plated in 96-well plates and incubated in a standard CO_2 incubator overnight. Cells were then incubated in 0.5% O_2 or 20% O_2 for 24 h. Adherent cells were assayed in the presence of 0.25% Triton X-100 and pro-protein convertase substrate at 37°C for 5 h. The data were normalized to cell density by parallel staining of another 96-well plate with crystal violet. Figure shows pooled results of five independent experiments (mean ± SEM). Data are normalized to results obtained from cells incubated under standard conditions (20% O_2) within each experiment. (A) Cells were plated at a density of 1.5×10^4 cells/well on day one [mean ± SEM: 119.8 ± 11.3%, 95% CI: (88.4, 151.2), p=0.0005, n=5]. (B) Cells were plated at a density of 2.0×10^4 cells/well on day one [mean ± SEM: 125.6 ± 16.6%, 95% CI: (79.5, 171.8), p=0.0017, n=5]. Statistically significant increase of pro-protein convertase activity in 0.5% O_2 relative to 20% $O_2$are indicated (*P<0.05; one-sample t-test).

Chapter 4

Discussion

Our laboratory's previous studies revealed that, upon exposure to hypoxia, tumour cells acquire resistance to the cytolytic activity of IL-2-activated lymphocytes, and that the mechanism of this hypoxia-mediated resistance to lysis involves the shedding of MIC, specifically MICA, from the tumour cell surface [57].

The main conclusion of this thesis is that the shedding of MICA in cells exposed to hypoxia is mediated by HIF-1. This conclusion is supported mainly by the results of experiments showing that knockdown of HIF-1α expression led to significant inhibition of hypoxia-induced shedding of MICA.

An objective of the present study was to identify molecules that are critical to the mechanism of hypoxia-induced shedding of MICA from the tumour cell surface; membrane-bound MICA expression was determined by flow cytometry. First, the hypoxia-induced MICA shedding was confirmed using MDA-MB-231 breast cancer cells. A mean 40% decrease in the level of surface MICA on MDA-MB-231 cells was observed after 24-h incubations in 0.5% O_2. Results revealed that the hypoxia-induced shedding of MICA from the tumour cell surface requires the expression of HIF-1. This conclusion is based on the results showing that intracellular HIF-1 levels increased under hypoxia, and that knockdown of HIF-1α mRNA using siRNA technology prevented this accumulation and blocked the shedding of MICA from the surface of MDA-MB-231 cells exposed to hypoxia. Furthermore, the role of the pro-protein convertase furin in the regulation of hypoxia-induced shedding of MICA was also explored. This was done to test the hypothesis that hypoxia increases MICA shedding in tumour cells via HIF-1-mediated activation of *fur* transcription. Interestingly, hypoxia did not increase the expression of furin in MDA-MB-231 cells exposed to hypoxia at the mRNA level nor at the protein level. This is despite a previous publication that reported a hypoxia-mediated up-regulation of furin expression in HepG2 cells [79]. However, in the present study, overall furin activity as measured using a furin activity assay (See Materials and Methods) was increased in cells exposed to hypoxia.

The findings of the present study indicate that HIF-1 may play an important role in tumour immune escape: membrane-bound MICA and NKG2D interactions have been proposed to participate in tumour immunosurveillance and MICA shedding from the tumour cell surface is now considered to be an important mechanism linked to tumour immune escape [20].

4.1 The significance of shedding of MICA

NKG2D-NKG2DL interactions can induce the activation of NK cells despite the presence of inhibitory signals induced by the expression of MHC class I molecules on target cells [21, 33]. NKG2D-NKG2DL interactions can also co-stimulate $CD8^+$ T cell activation [21]. In the present study, an average 40% decrease was observed in the levels of membrane-bound MICA on MDA-MB-231 cell surface after a 24-h incubation in

0.5% O_2. Since MICA is an important ligand for NKG2D, this decreased expression likely results in a net attenuation of NK cell activation. Furthermore, soluble MICA released from the tumour cell surface can bind to the NKG2D receptor, thereby blocking the NKG2D-NKG2DL interaction between immune effector cells and tumour cells [20]. Moreover, soluble MICA has been shown to down-regulate NKG2D expression in effector cells [20, 57]. Thus, it is now well accepted that the shedding of MICA impairs the ability of NK cells to eliminate primary tumours and metastases. The clinical significance of MICA shedding has been proven by various clinical studies. High levels of soluble MICA were detected in sera of patients suffering from different types of cancer, including breast and lung cancer, leukemia, pancreatic carcinomas, hepatocellular cancer and colon carcinoma [28, 38-41]. There is also evidence that soluble MICA is an independent marker of progression for many early-stage cancers, such as gastrointestinal, breast, and prostate carcinoma [20, 42]. Thus the hypoxia-mediated decreased expression of MICA on the tumour cell surface may have important clinical implications; consequently, HIF-1, which is required for the hypoxia-mediated shedding of MICA, likely plays an important role in tumour immune escape.

4.2 Potential 'Sheddases' involved in the release of MICA from the tumour cell surface

It was reported that the shedding of MICA from the cell surface requires the cleavage of the extracellular domains of MICA through a process involving metalloproteinase activity [28]. A recent study revealed that MICA shedding by tumour cells requires the action of ADAM-10 and ADAM-17, two members of the “a disintegrin and metalloproteinase” (ADAM) family of metalloproteinases [43]. Other studies showed that the cell surface endoplasmic reticulum protein 5 (ERp5) is also required for MICA shedding through the formation of mixed disulfide complexes that release MICA [44]. In support of this finding, a recent report demonstrated a correlation between MICA and ERp5 levels in the sera of patients with multiple myeloma [87]. An important future goal arising from the present study is to determine which sheddases are involved in the hypoxia-mediated release of MICA from tumour cells.

4.3 The expression of other NKG2D ligands under hypoxia

The MIC molecules are a family of NKG2D ligands. The Retinoic Acid Early Transcript (RAET) family is another class of NKG2D ligands; RAET was initially referred to as the UL16-binding proteins (ULBPs) [20]. RAET proteins are also rarely detectable on the surface of healthy cells and tissues, but are frequently expressed by tumour cell lines and in tumour tissues including leukemia, gliomas and melanomas [20, 26-28].Thus it would be very interesting to determine whether hypoxia can cause the shedding of RAET members on the tumour cell surface, and if so, whether the mechanism of shedding of RAET molecules is similar to the one responsible for the hypoxia-mediated shedding of MICA described in the present study.

4.4 Extended discussion on NKG2D in tumour surveillance

NKG2D-deficient mice have been used to study the significance of NKG2D-mediated immunity during tumourigenesis. These mice were crossed to transgenic adenocarcinoma of the mouse prostate (TRAMP) mice that spontaneously develop prostatic adenocarcinoma. This was done to generate male NKG2D-deficient TRAMP mice as well as NKG2D wild-type TRAMP littermates. Results showed that NKG2D-deficient TRAMP mice are three times more likely than wild-type NKG2D TRAMP littermates to develop highly malignant, early-arising prostate adenocarcinoma [88].

Interestingly, an in vitro study showed that exposure of purified NK cells to NKG2D ligand-expressing targets leads only to low levels of target cell killing. However, culture of NK cells in the presence of interleukin (IL)-15 or high doses of IL-2 significantly increased NKG2D-mediated killing of tumour targets [20]. Our laboratory’s previous studies revealed that, upon exposure to hypoxia, tumour cells acquire resistance to the cytolytic activity of IL-2-activated lymphocytes [57]. Future studies are required to determine whether HIF-1 knockdown can rescue the cytolytic effect of IL-2-activated lymphocytes against cancer cells exposed to hypoxia. This could confirm the conclusion that HIF-1 plays an important role in tumour immune escape by mediating hypoxia-induced MICA shedding from the tumour cell surface.

4.5 Furin expression vs. furin activity under hypoxia

Among the PC convertases, furin was the first identified and has been the most extensively studied. Furin mRNA is detected in all tissues and cell lines examined so far, and furin protein is mainly localized to the trans-Golgi network [77]. It has been reported that furin mRNA expression is up-regulated approximately 18-fold in human hepatoma HepG2 cells exposed to 24-h hypoxia, and this enhanced mRNA expression is mediated by HIF-1 [79]. However, in the present study, high levels of furin protein were present in MDA-MB-231 cells even when these cells were cultured under standard conditions (20% O_2), and no increase in furin expression was observed in cells exposed to 24-h hypoxia, either at the mRNA level or at the protein level. One potential explanation for this lack of up-regulation by hypoxia is that furin expression in these cells may already be maximal under standard culture conditions, and therefore hypoxia is unable to further increase furin expression. This explanation is supported by a study of furin levels in ovarian cancer. In that study, furin protein expression was clearly found in all of the different ovarian cancer cell lines but not in cells derived from the normal ovarian surface epithelium; increased expression of furin was correlated with decreased survival [89]. It has also been reported that furin is over-expressed in colon, head and neck, and breast cancers [89].

Although furin mRNA and protein expression were not increased by hypoxia in the present study, overall pro-protein convertase activity was significantly elevated in MDA-MB-231 cells exposed to hypoxia. Human furin is initially synthesized as 100-kD profurin, which is then converted into 94-kD forms by intro-molecular autocatalytic cleavage of the pro-peptide. However, even after its cleavage, the pro-peptide remains associated with the mature furin moiety and functions as a potent auto-inhibitor of furin [78]. Upon exposure of the latent form of furin to low pH and Ca^{2+}, the pro-peptide is further cleaved and released, generating active furin [78]. Meanwhile, cellular adaptation to hypoxia is accompanied by a decreased intracellular pH resulting from cells switching from oxygen-dependent tricarboxylic acid (TCA) cycle and oxidative phosphorylation to glucose consumption and lactic acid production [45]. Therefore, the possible explanation for the present results is that hypoxia reduces the intracellular pH level, thereby inducing the release of the propeptide from latent furin zymogen, resulting in an increase of overall furin activity under hypoxia.

4.6 Furin is involved in hypoxia-induced shedding of MICA and tumour immune escape

To determine whether furin expression and activity are required for the hypoxia-induced shedding of MICA and tumour immune escape, furin expression was knocked down in our laboratory by introducing furin siRNA into MDA-MD-231 cells, and furin activity was inhibited by incubating cells with the furin protease inhibitor decanoyl-Arg-Val-Lys-Arg-chloromethylketone (CMK). Results showed that knockdown of furin expression with siRNA or inhibition of furin activity with CMK blocked the hypoxia-induced MICA shedding, and interfered with hypoxia-induced resistance to the cytolytic activity of IL-2-activated lymphocytes (Nianping Hu, D.R.Siemens and C.H.Graham, unpublished).

While furin expression and activity are required for the hypoxia-induced shedding of MICA, the finding that hypoxia did not up-regulate furin expression in the MDA-MB-231 cells in the present study indicates that furin was not likely the primary mediator of the hypoxia-induced shedding of MICA. Recent studies revealed that the sheddases ADAM-10 and ADAM-17 are responsible for the shedding of MICA [43] and can be up-regulated by hypoxia [90]. Thus, it is possible that the shedding of MICA under hypoxic conditions is due to a HIF-1-mediated up-regulation of ADAM-10 and ADAM-17 (Figure 4.1). Future studies are required to test this hypothesis and to determine the HIF-1 target genes involved in the hypoxia-induced MICA shedding pathway and hypoxia-induced immune escape.

In summary, the results of the present study support a role for hypoxia in cancer immune escape and provide evidence of a mechanism of hypoxia-mediated immune escape involving HIF-1 activity.

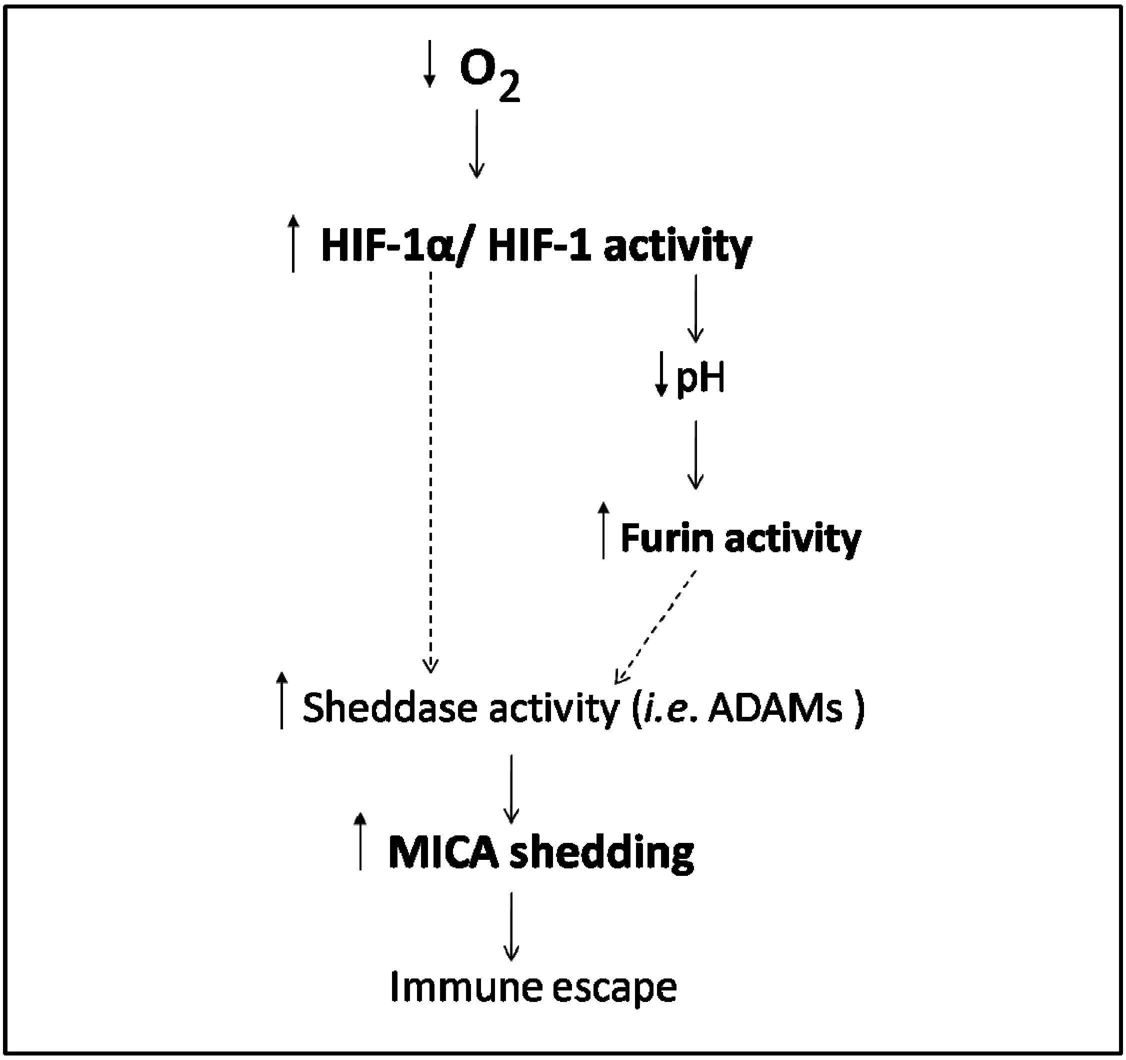

Figure 4.1 Modified proposed mechanism of hypoxia-mediated immune escape.

Chapter 5

Future directions

1. To determine whether HIF-1α knockdown can rescue the lytic effect of IL-2-activated lymphocytes against cancer cells exposed to hypoxia.

2. To determine whether the shedding of MICA under hypoxic conditions is due to a HIF-1-mediated up-regulation of ADAM-10 and ADAM-17 activity.

3. To determine whether hypoxia can induce the shedding of RAET members on the tumour cell surface, and if so, whether the mechanism of shedding of RAET NKG2D ligands is similar to the one responsible for the hypoxia-mediated shedding of MICA described in the present study.

References

[1] Dunn GP, Koebel CM, Schreiber RD. Interferons, immunity and cancer immunoediting. Nat Rev Immunol 2006; 6: 836-848.

[2] Klein G. Immunological surveillance against neoplasia. Harvey Lect 1973; 71-102.

[3] Stutman O. Tumor development after 3-methylcholanthrene in immunologically deficient athymic-nude mice. Science 1974; 183:534-536.

[4] Dunn GP, Bruce AT, Ikeda H, Old LJ, Schreiber RD. Cancer immunoediting: from immunosurveillance to tumor escape. Nat Immunol 2002; 11:991-998.

[5] Dunn GP, Old LJ, Schreiber RD. The Three Es of Cancer Immunoediting. Annu Rev Immunol 2004; 22:329-360.

[6] Dunn GP, Old LJ, Schreiber RD. The Immunobiology of Cancer Immunosurveillance and Immunoediting. Immunity 2004; 21:137-148.

[7] Shankaran V, Ikeda H, Bruce AT, White JM, Swanson PE, Old LJ, Schreiber RD. IFN-γ and lymphocytes prevent primary tumour development and shape tumour immunogenicity. Nature 2001; 410:1107-1111.

[8] Smyth MJ, Thia KY, Street SE, Creteny E, Trapani JA, Taniquchi M, Kawano T, Pelikan sb, Crowe NY, Godfrey DI. Differential Tumor Surveillance by Natural Killer (NK) and NKT Cells. J Exp Med 2000; 191:661-668.

[9] Street SE, Trapani JA, MacGregor D, Smyth MJ. Suppression of Lymphoma and Epithelial Malignancies Effected by Interferon-γ. J Exp Med 2002; 196:129-134.

[10] Raulet DH. Roles of the NKG2D immunoreceptor and its ligands. Nat Rev Immunol 2003; 3:781-790.

[11] Dunn GP, Bruce AT, Sheehan KC, Shankaran V, Uppaluri R, Bui JD, Diamond MS, Koebel CM, Arthur C, White JM, Schreiber RD. A critical function for type I interferons in cancer immunoediting. Nat Immunol 2005; 6:722-729.

[12] Houchins JP, Yabe T, McSherry C, Miyokawa N, Bach FH. Isolation and characterization of NK cell or NK/T cell-specific cDNA clones. J Mol Cell Immunol 1990; 4:295-306.

[13] Wu J, Song Y, Bakker AB, Bauer S, Spies T, Lanier LL, Philips JH. An Activating Immunoreceptor Complex Formed by NKG2D and DAP10. Science 1999; 285:730-732.

[14] Pillarisetty VG, Shah AB, Miller G, Bleier JI, DeMatteo RP. Liver Dendritic Cells Are Less Immunogenic Than Spleen Dendritic Cells because of Differences in Subtype Composition. J Immunol 2004; 172:1009-1017.

[15] Chan CW, Crafton E, Fan HN, Flook J, Yoshimura K, Skarica M, Brockstedt D, Dubensky TW, Stins MF, Lanier LL, Pardoll DN, Housseau F. Interferon-producing killer dendritic cells provide a link between innate and adaptive immunity. Nat Med 2006; 12:207-213.

[16] Taieb J, Chaput N, Menard C, Apetoh L, Ullrich E, Bonmort M, Pequiqnot M, et al. A novel dendritic cell subset involved in tumor immunosurveillance. Nat Med 2006; 12:214-219.

[17] Vosshenrich CA, Lesjean-Pottier S, Hasan M, Richard-Le GO, Crocuff E, Mandelboim O, Di Santo JP . CD11c^{lo}B220+ interferon-producing killer dendritic cells are activated natural killer cells. J Exp Med 2007; 204:2569-2578.

[18] Ehrlich LI, Ogasawara K, Hamerman JA, Takaki R, Zingoni A, Allison JP, Lanier LL. Engagement of NKG2D by Cognate Ligand or Antibody Alone Is Insufficient

to Mediate Costimulation of Human and Mouse CD8+ T Cells. J Immunol 2005; 174:1922-1931.

[19] Groh V, Smythe K, Dai Z, Spies T. Fas ligand-mediated paracrine T cell regulation by the receptor NKG2D in tumor immunity. Nat Immunol 2006; 7:755-762.

[20] Nausch N, Cerwenka A. NKG2D ligands in tumor immunity. Oncogene 2008; 27:5944-5958.

[21] Bauer S, Groh V, Wu J, Seteinle A, Philips JH, Lanier LL, Spies T. Activation of NK Cells and T Cells by NKG2D, a Receptor for Stress-Inducible MICA. Science 1999; 285:727-729.

[22] Cerwenka A, Bakker AB, McClanahan T, Wagner J, Wu J, Phillips JH, Lanier LL. Retinoic Acid Early Inducible Genes Define a Ligand Family for the Activating NKG2D Receptor in Mice. Immunity 2000; 12:721-727.

[23] Diefenbach A, Jamieson AM, Liu SD, Shastri N, Raulet DH. Ligands for the murine NKG2D receptor: expression by tumor cells and activation of NK cells and macrophages. Nat Immunol 2000; 1:119-126.

[24] Radosavljevic M, Cuillerier B, Wilson MJ, Clément O, Wicker S, Gilfillan S, Beck S, Trowsdale J, Bahram S. A Cluster of Ten Novel MHC Class I Related Genes on Human Chromosome 6q24.2-q25.3. Genomics 2002; 79:114-123.

[25] Bahram S, Bresnahan M, Geraghty DE, Spies T. A second lineage of mammalian major histocompatibility complex class I genes. Proc Natl Acad Sci U S A 1994; 91:6259-6263.

[26] Pende D, Rivera P, Marcenaro S, Chang CC, Biassoni R, Conte R, Kubin M, Cosman D, Ferrone S, Moretta L, Moretta A. Major Histocompatibility Complex Class I-related Chain A and UL16-Binding Protein Expression on Tumor Cell Lines of Different Histotypes: Analysis of Tumor Susceptibility to NKG2D-dependent Natural Killer Cell Cytotoxicity. Cancer Res 2002; 62:6178-6186.

[27] Friese MA, Platten M, Lutz SZ, Naumann U, Aulwurm S, Bischof F, Bühring HJ, Dichgans J, Rammensee HG, Steinle A, Weller M . MICA/NKG2D-Mediated Immunogene Therapy of Experimental Gliomas. Cancer Res 2003; 63:8996-9006.

[28] Salih HR, Antropius H, Gieseke F, Lutz SZ, Kanz L, Rammensee HG, Steinle A. Functional expression and release of ligands for the activating immunoreceptor NKG2D in leukemia. Blood 2003; 102:1389-1396.

[29] Groh V, Rhinehart R, Secrist H, Bauer S, Grabstein KH, Spies T. Broad tumor-associated expression and recognition by tumor-derived γδ T cells of MICA and MICB. Proc Natl Acad Sci U S A 1999; 96:6879-6884.

[30] Vetter CS, Groh V, thor Straten P, Spies T, Bröcker EB, Becker JC. Expression of Stress-induced MHC Class I Related Chain Molecules on Human Melanoma. J Invest Dermatol 2002; 118:600-605.

[31] Watson NF, Spendlove I, Madjd Z, McGilvray R, Green AR, Ellis IO, Scholefield JH, Durrant LG. Expression of the stress-related MHC class I chain-related protein MICA is an indicator of good prognosis in colorectal cancer patients. Int J Cancer 2006; 118:1445-1452.

[32] Castriconi R, Dondero A, Negri F, Bellora F, Nozza P, Carnemolla B, Raso A, Moretta L, Moretta A, Bottino C. Both CD133+ and CD133-dulloblastoma cell lines express ligands for triggering NK receptors and are susceptible to NK-mediated cytotoxicity. Eur J Immunol 2007; 37:3190-3196.

[33] Cerwenka A, Baron JL, Lanier LL. Ectopic expression of retinoic acid early inducible-1 gene (RAE-1) permits natural killer cell-mediated rejection of a MHC class I-bearing tumor in vivo. Proc Natl Acad Sci U S A 2001; 98:11521-11526.

[34] Kindt TJ, et al (2007). Kuby Immunology. 6th Ed. New York: Sara Tenney.

[35] Venkataraman GM, Suciu D, Groh V, Boss JM, Spies T. Promoter Region Architecture and Transcriptional Regulation of the Genes for the MHC Class I-Related Chain A and B Ligands of NKG2D. J Immunol 2007; 178:961-969.

[36] Angel P, Szabowski A, Schorpp-Kistner M. Function and regulation of AP-1 subunits in skin physiology and pathology. Oncogene 2001; 20:2413-2423.

[37] Gasser S, Orsulic S, Brown EJ, Raulet DH. The DNA damage pathway regulates innate immune system ligands of the NKG2D receptor. Nature 2005; 436:1186-1190.

[38] Groh V, Wu J, Yee C, Spies T. Tumour-derived soluble MIC ligands impair expression of NKG2D and T-cell activation. Nature 2002; 419:734-738.

[39] Märten A, von Lilienfeld-Toal M, Büchler MW, Schmidt J. Soluble MIC is elevated in the serum of patients with pancreatic carcinoma diminishing gammadelta T cell cytotoxicity. Int J Cancer 2006; 119:2359-2365.

[40] Jinushi M, Takehara T, Tatsumi T, Kanto T, Groh V, Spies T, Kimura R, Miyagi T, Mochizuki K, Sasaki Y, Hayashi N. Expression and role of MICA and MICB in human hepatocellular carcinomas and their regulation by retinoic acid. Int J Cancer 2003; 104:354-361.

[41] Doubrovina ES, Doubrovin MM, Vider E, Sisson RB, O'Reilly RJ, Dupont B, Vyas YM. Evasion from NK Cell Immunity by MHC Class I Chain-Related Molecules Expressing Colon Adenocarcinoma. J Immunol 2003; 171:6891-6899.

[42] Yokoyama WM. Immunology: Catch us if you can. Nature 2002; 419:679-680.

[43] Waldhauer I, Goehlsdorf D, Gieseke F, Weinschenk T, Wittenbrink M, Ludwig A, Stevanovic S, Rammensee HG, Steinle A. Tumor-Associated MICA Is Shed by ADAM Proteases. Cancer Res 2008; 68:6368-6376.

[44] Kaiser BK, Yim D, Chow IT, Gonzalez S, Dai Z, Mann HH, Strong RK, Groh V, Spies T. Disulphide-isomerase-enabled shedding of tumour-associated NKG2D ligands. Nature 2007; 447:482-486.

[45] Zhou J, Schmid T, Schnitzer S, Brüne B. Tumor hypoxia and cancer progression. Cancer Letters 2006; 237:10-21.

[46] Brown JM, Wilson WR. Exploiting tumour hypoxia in cancer treatment. Nat Rev Cancer 2004; 4:437-447.

[47] Vaupel P, Mayer A. Hypoxia in cancer: significance and impact on clinical outcome. Cancer Metastasis Rev 2007; 26:225-239.

[48] Brizel DM, Sibley GS, Prosnitz LR, Scher RL, Dewhirst MW. Tumor hypoxia adversely affects the prognosis of carcinoma of the head and neck. Int J Radiat Oncol Biol Phys 1997; 38:285-289.

[49] Lartigau E, Randrianarivelo H, Avril MF, Margulis A, Spatz A, Eschwège F, Guichard M. Intratumoral oxygen tension in metastatic melanoma. Melanoma Res 1997; 7:400-406.

[50] Brizel DM, Scully SP, Harrelson JM, Layfield LJ, Bean JM, Prosnitz LR, Dewhirst MW. Tumor Oxygenation Predicts for the Likelihood of Distant Metastases in Human Soft Tissue Sarcoma. Cancer Res1996; 56:941-943.

[51] Hockel M, Schlenger K, Aral B, Mitze M, Schaffer U, Vaupel P. Association between Tumor Hypoxia and Malignant Progression in Advanced Cancer of the Uterine Cervix. Cancer Res 1996; 56: 4509-4515.

[52] Movsas B, Chapman JD, Greenberg RE, Hanlon AL, Horwitz EM, Pinover WH, Stobbe C, Hanks GE. Increasing levels of hypoxia in prostate carcinoma correlate significantly with increasing clinical stage and patient age. Cancer 2000; 89:2018-2024.

[53] Movsas B, Chapman JD, Horwitz EM, Pinover WH, Greenberg RE, Hanlon AL, Iyer R, Hanks GE. Hypoxic regions exist in human prostate carcinoma. Urology 1999; 53:11-18.

[54] Teicher BA, Lazo JS, Sartorelli AC. Classification of Antineoplastic Agents by their Selective Toxicities toward Oxygenated and Hypoxic Tumor Cells. Cancer Res 1981; 41:73-81.

[55] Comerford KM, Wallace TJ, Karhausen J, Louis NA, Montalto MC, Colgan SP. Hypoxia-inducible Factor-1-dependent Regulation of the Multidrug Resistance (MDR1) Gene. Cancer Res 2002; 62:3387-3394.

[56] Wartenberg M, Gronczynska S, Bekhite MM, Saric T, Niedermeier W, Hescheler J, Sauer H. Regulation of the multidrug resistance transporter P-glycoprotein in multicellular tumor spheroids by hypoxia-inducible factor-1 and reactive oxygen species. FASEB J, 2003; 17:503-505.

[57] Siemens DR, Hu N, Sheikhi AK, Chung E, Frederiksen LJ, Pross H, Graham CH.Hypoxia Increases Tumor Cell Shedding of MHC Class I Chain-Related Molecule: Role of Nitric Oxide. Cancer Res 2008; 68:4746-4753.

[58] Hirsilä M, Koivunen P, Günzler V, Kivirikko KI, Myllyharju J. Characterization of the human prolyl 4-hydroxylases that modify the hypoxia-inducible factor HIF. J Biol Chem 2003; 278:30772-30780.

[59] Pugh CW, Ratcliffe PJ. The von Hippel-Lindau tumor suppressor, hypoxia-inducible factor-1 (HIF-1) degradation, and cancer pathogenesis. Semin Cancer Biol 2003; 13:83-89.

[60] Ke Q, Costa M. Hypoxia-Inducible Factor-1 (HIF-1). Mol Pharmacol 2006; 70:1469-1480.

[61] Minet E, Michel G, Mottet D, Raes M, Michiels C. Transduction pathways involved in Hypoxia-Inducible Factor-1 phosphorylation and activation. Free Radic Biol Med 2001; 31:847-855.

[62] Suzuki H, Tomida A, Tsuruo T. Dephosphorylated hypoxia-inducible factor 1alpha as a mediator of p53-dependent apoptosis during hypoxia. Oncogene 2001; 20:5779-5788.

[63] Semenza GL, Nejfelt MK, Chi SM, Antonarakis SE. Hypoxia-inducible nuclear factors bind to an enhancer element located 3' to the human erythropoietin gene. Proc Natl Acad Sci U S A 1991; 88:5680-5684.

[64] Rolfs A, Kvietikova I, Gassmann M, Wenger RH. Oxygen-regulated Transferrin Expression Is Mediated by Hypoxia-inducible Factor-1. J Biol Chem 1997; 272:20055-20062.

[65] Neufeld G, Cohen T, Gengrinovitch S, Poltorak Z. Vascular endothelial growth factor (VEGF) and its receptors. FASEB J 1999; 13:9-22.

[66] Conway EM, Collen D, Carmeliet P. Molecular mechanisms of blood vessel growth. Cardiovasc Res 2001; 49:507-521.

[67] Jośko J, Gwóźdź B, Jedrzejowska-Szypułka H, Hendryk S. Vascular endothelial growth factor (VEGF) and its effect on angiogenesis. Med Sci Monit 2000; 6:1047-1052.

[68] Dang CV, Semenza GL. Oncogenic alterations of metabolism. Trends Biochem Sci 1999; 24:68-72.

[69] Seagroves TN, Ryan HE, Lu H, Wouters BG, Knapp M, Thibault P, Laderoute K, Johnson RS. Transcription Factor HIF-1 Is a Necessary Mediator of the Pasteur Effect in Mammalian Cells. Mol Cell Biol 2001; 21:3436-3444.

[70] Wenger RH. Cellular adaptation to hypoxia: O2-sensing protein hydroxylases, hypoxia-inducible transcription factors, and O2-regulated gene expression. FASEB J 2002; 16:1151-1162.

[71] Feldser D, Agani F, Iyer NV, Pak B, Ferreira G, Semenza GL. Reciprocal Positive Regulation of Hypoxia-inducible Factor 1-α and Insulin-like Growth Factor 2. Cancer Res 1999; 59:3915-3918.

[72] Krishnamachary B, Berg-Dixon S, Kelly B, Agani F, Feldser D, Ferreira G, Iyer N, LaRusch J, Pak B, Taghavi P, Semenza GL. Regulation of Colon Carcinoma Cell Invasion by Hypoxia-Inducible Factor 1. Cancer Res 2003; 63:1138-1143.

[73] Seidah NG, Khatib AM, Prat A. The proprotein convertases and their implication in sterol and/or lipid metabolism. Biol Chem 2006; 387: 871-877.

[74] Seidah NG, Mayer G, Zaid A, Rousselet E, Nassoury N, Poirier S, Essalmani R, Prat A. The activation and physiological functions of the proprotein convertases. Int J Biochem Cell Biol 2008; 40:1111-1125.

[75] Bassi DE, Fu J, Lopez de Cicco R, Klein-Szanto AJ. Proprotein Convertases: "Master Switches" in the Regulation of Tumor Growth and Progression. Mol Carcinog 2005; 44:151-161.

[76] Scamuffa N, Siegfried G, Bontemps Y, Ma L, Basak A, Cherel G, Calvo F, Seidah NG, Khatib AM. Selective inhibition of proprotein convertases represses the metastatic potential of human colorectal tumor cells. J Clin Invest 2008; 118: 352-363.

[77] Molloy SS, Thomas L, VanSlyke JK, Stenberg PE, Thomas G. Intracellular trafficking and activation of the furin proprotein convertase: localization to the TGN and recycling from the cell surface. EMBO J 1994; 13:18–33.

[78] Nakayama K. Furin: a mammalian subtilisin/Kex2p-like endoprotease involved in processing of a wide variety of precursor proteins. Biochem J 1997; 327:625-635.

[79] McMahon S, Grondin F, McDonald PP, Richard DE, Dubois CM. Hypoxia-enhanced Expression of the Proprotein Convertase Furin Is Mediated by Hypoxia-inducible Factor-1: IMPACT ON THE BIOACTIVATION OF PROPROTEINS. J Biol Chem 2005; 280:6561-6569.

[80] Fang Y, Sullivan R, Graham CH. Confluence-dependent resistance to doxorubicin in human MDA-MB-231 breast carcinoma cells requires hypoxia-inducible factor-1 acitity. Exp Cell Res 2007; 313:867-877

[81] Stone KR, Mickey DD, Wunderli H, Mickey GH, Paulson DF. Isolation of a human prostate carcinoma cell line (DU 145). Int J Cancer 1978; 21: 274-281

[82] Nupponen NN, Hyytinen ER, Kallioniemi AH, Visakorpi T. Genetic alterations in prostate cancer cell lines detected by comparative genomic hybridization. Cancer Genet Cytogenet 1998; 101:53-7.

[83] Yuasa K, Suzue K, Nagahama M, Matsuda Y, Tsuji A. Transcriptional regulation of subtilisin-like proprotein convertase PACE4 by E2F: Possible role of E2F-mediated upregulation of PACE4 in tumor progression. Gene 2007; 402:103–110

[84] Molloy SS, Bresnahan PA, Leppla SH, Klimpel KR, Thomas G. Human Furin Is a Calcium-dependent Serine Endoprotease That Recognizes the Sequence Arg-X-X-Arg and Efficiently Cleaves Anthrax Toxin Protective Antigen. J Biol Chem 1992; 267:16396-16402

[85] Leitlein J, Aulwurm S, Waltereit R, Naumann U, Wagenknecht B, Garten W, Weller M, Platten M. Processing of Immunosuppressive Pro-TGF-β1,2 by Human Glioblastoma Cells Involves Cytoplasmic and Secreted Furin-Like Proteases. J Immunol 2001; 166: 7238–7243.

[86] Ornatowski W, Poschet JF, Perkett E, Taylor-Cousar JL, Deretic V. Elevated furin levels in human cystic fibrosis cells result in hypersusceptibility to exotoxin A–induced cytotoxicity. J Clin Invest 2007; 117:3489–3497.

[87] Jinushi M, Vanneman M, Munshi NC, Tai YT, Prabhala RH, Ritz J, Neuberg D, Anderson KC, Carrasco DR, Dranoff G. MHC class I chain-related protein A antibodies and shedding are associated with the progression of multiple myeloma. Proc Natl Acad Sci U S A 2008; 105:1285–1290

[88] Guerra N, Tan YX, Joncker NT, Choy A, Gallardo F, Xiong N, Knoblaugh S, Cado D, Greenberg NM, Raulet DH. NKG2D-Deficient Mice Are Defective in Tumor Surveillance in Models of Spontaneous Malignancy. Immunity 2008; 28: 571–580

[89] Page RE, Klein-Szanto AJ, Litwin S, Nicolas E, Al-Jumaily R, Alexander P, Godwin AK, Ross EA, Schilder RJ, Bassi DE. Increased expression of the pro-protein convertase furin predicts decreased survival in ovarian cancer. Cell Oncol 2007; 29: 289-299

[90] Charbonneau M, Harper K, Grondin F, Pelmus M, McDonald PP, Dubois CM. Hypoxia-inducible Factor Mediates Hypoxic and Tumor Necrosis Factor α-induced Increases in Tumor Necrosis Factor-α Converting Enzyme/ADAM17 Expression by Synovial Cells. J Biol Chem 2007; 282:33714-33724.